THE ASTROPHYSICAL JOURNAL SUPPLEMENT SERIES, 51:211–248, 1983 February

CHEMICAL COMPOSITIONS OF PLANETARY NEBULAE

LAWRENCE H. ALLER
Department of Astronomy, University of California, Los Angeles
AND
STANLEY J. CZYZAK
Department of Astronomy, Ohio State University
Received 1982 April 26; accepted 1982 August 4

ABSTRACT

Image-tube scanner measurements, supplemented where possible by *IUE* data, are analyzed and reassessed as necessary to establish chemical compositions of 41 planetary nebulae. The objects cover a large range in surface brightness, structural complexity, and excitation. Two methods are employed. In one, theoretical models are calculated to represent individual line intensities and excitation-sensitive ratios such as [O II]/[O III], He II/He I, and [Ne V]/[Ne III]. The "model abundances" thus derived correspond to the best fit of observed and calculated intensities within the framework imposed by the basic assumptions. For many objects fairly satisfactory representations are possible, but for a few nebulae, such as Hu 1–2 and NGC 2371–72, no satisfactory model could be obtained—at least none involving a simple geometry. Only the general level of excitation can be reproduced. In the second method we determine for each nebula the diagnostics, N_ε, T_ε, and employ them to calculate the concentration, $N(X_i)/N(\mathrm{H}+)$, for each observed ion. We try to calculate a theoretical model that gives satisfactory values of the observed intensities and the aforementioned excitation-sensitive ratios to obtain ionization correction factors which are then applied to the ionic concentrations to get total abundances. This procedure, applied, e.g., by Shields *et al.* to NGC 2440, is the one we favor. The mean logarithmic deviations between abundances derived by the two methods, $\Delta = \langle |\ln N_{\mathrm{el}}(\mathrm{ICF})/N_{\mathrm{el}}(\mathrm{model})| \rangle$, is of the order of 0.10, except for N and S where Δ tends to be larger, primarily for reasons outlined in the text. The quality of the individual nebular analyses varies, depending on the completeness and accuracy of the observational data and the complexity of the nebular structure. We assign quality estimates for each element in each nebula and try to give an overall reliability index to each object. Thus, the confidence with which we can speak of the chemical composition of a nebula may vary over a fair range.

The mean logarithmic abundances found for this sample of nebulae plus those individual objects previously reported are as follows:

He	11.04	O	8.64	Na	6.18	Ar	6.43
C	8.89	F	4.6:	S	7.00	K	4.95
N	8.26	Ne	8.03	Cl	5.22	Ca	5.03.

Since our sample includes many objects of high surface brightness, the mean chemical compositions must reflect this bias. Detailed discussion and comparison with results of other works is deferred to a second paper.

Subject headings: nebulae: abundances — nebulae: planetary

I. INTRODUCTION

Chemical compositions of planetary nebulae have been studied systematically from two points of view. In one we stress the use of planetary nebulae as tools for galactic structure. We pick them to cover as large a range as possible in distance from the galactic center, or over a big range in kinematical characteristics, or both. Such studies by Torres-Peimbert and Peimbert (1977, hereafter TPP), Barker (1978*a*, *b*, *c*), and Kaler (1978*a*, *b*, *c*, 1979) and investigations of halo objects and nebulae at high galactic latitudes (see, e.g., Peimbert 1973; Miller 1969) have been concerned with a small number of chemical elements in a widely distributed population.

In the second point of view, we stress the basic physics and detailed structures of individual objects. An example in point is the very elaborate, careful, and painstaking analysis of NGC 7662 carried out by Harrington *et al.* (1982). They were concerned with the abundances of He, C, N, O, Ne, Mg, Si, and S. For NGC 2440 Shields *et al.* (1981) employed models as an interpolation device. This method has also been applied by Aller *et al.* (1979, 1981*a*, *b*, *c*) and is the one favored here. Beck *et al.* (1981) have used the procedure described in this paper to establish abundances of neon, argon, and sulfur. They used infrared as well as optical region data. In planetary nebulae whose spectra have been studied in considerable detail, some information is available for elements such as fluorine, sodium, potassium, and calcium.

How good are planetary nebulae as probes of the chemical composition of the interstellar medium at the time the parent stars were formed, either in our own or other galaxies? Kaler (1978*a*, *b*, *c*), TPP (1977), Barker (1978*a*, *b*, *c*) Aller (1976), Peimbert and Serrano (1980), and others have examined how chemical composition changes as a function of distance from the galactic center. The answer depends on the elements involved and the extent to which products of nuclear processing get conveyed to surface layers. These effects depend on the mass of the progenitor star. Most planetary nebulae probably do not generate new nuclides (Peimbert and Serrano 1980); in their scenario, only those with progenitor stars more massive than 2.4 solar masses ejected processed material.

The elements that get processed substantially are those involved in the CNO cycle, particularly carbon and nitrogen. It is precisely these elements that offer severe abundance determination problems. For the resolution of this difficulty we particularly need *IUE* data for the lines of carbon and nitrogen ions. A large body of data (see Kaler 1978*a*, *b*, *c*) suggests that the abundances of neon, sulfur, chlorine, and argon are not much affected by nuclear processes in planetary nebulae progenitors. The proportions of these elements probably truly reflect the composition of the medium from which the precursor stars were formed.

It is well established that pronounced chemical composition differences do exist (see, e.g., Peimbert 1981). Some objects (e.g., NGC 6302) are definitely nitrogen rich, while others are especially rich in carbon. Current opinion is that nitrogen-rich objects have simply conveyed products of the CNO cycle to the surface. The CNO cycle equilibrium favors nitrogen at the expense of carbon.

On the other hand, carbon enrichment would imply that helium-burning products reached the surface. Many have suggested that the immediate precursors of planetary nebulae are carbon stars. Direct evidence for this conclusion is impressive: (1) frequent excess of carbon in planetary nebular envelopes; (2) frequent appearances in infrared emission, implying solid grains which are often interpreted as solid carbon particles; (3) presence of Wolf-Rayet central stars of the carbon sequence; (4) spatial distribution of carbon stars that resembles that of planetary nebulae. A popular scenario is that when a red giant star evolves, it may change from an M star to a carbon star and then evolve into a planetary nebula. If this schedule was followed in every instance, then all planetary nebulae should be carbon rich. It is not clear that this situation always occurs, although the C/O ratio is quite often enhanced.

On the other hand, Kaler (1980) concludes that all planetary nebulae with high O/H ratios favor the galactic disk. Upon dividing his sample of 97 planetaries into relative age groups, he found the mean O/H ratio to increase as younger and younger groups were sampled. This increase in O/H ratio by a factor of 5 or 10 after the formation of the early halo objects could be attributed to a gradual rise in the heavier element content of the galaxy. The O/H ratio rose rapidly from old to intermediate halo populations and then at a lower rate among the disk objects.

Current belief is that progenitor stars are not so massive as to manufacture neon and heavier elements in their interior and then convey them to the surface. The abundances of these elements must generally reflect those in the interstellar medium at the time the progenitor stars were formed.

There remains the engaging question as to how well current scenarios of stellar evolution quantitatively fit observed enhancements in planetary nebulae. How well can one correlate the required excesses of C, N, etc., with theoretical stellar evolution tracks? Discussions have been given, e.g., by Becker and Iben (1980), Renzini and Voli (1981), and Peimbert (1981).

Nearby external galaxies may offer some interesting clues. An example in point is offered by the few planetary nebulae so far studied in the Magellanic Clouds (Osmer 1976; Dufour and Killen 1977; Aller *et al.* 1981*c*). Maran *et al.* (1982) find the carbon abundance in these objects to be enhanced definitely with respect to the H II region. In the Large Magellanic Cloud objects, neon and argon tend to have comparable abundances in planetary nebulae and in H II regions. In seven planetary nebulae in the Small Magellanic Cloud, Aller *et al.* (1981*c*) found that N and He tend to be enhanced, but O, Ne, S, and Ar all appear to have roughly comparable abundances to those found in H II regions. Thus, planetary nebulae would appear to be carbon suppliers for the Magellanic Clouds, but heavier elements must come from more massive stars and supernovae. Yet the total amount of material supplied to the interstellar medium by carbon stars via planetary nebulae must be small compared with that supplied by these massive stars and supernovae; otherwise, we would expect carbon to exceed oxygen in abundance.

The present program involves a study of some 50-plus planetary nebulae, results for 41 of which are presented here. Most of them have high surface brightnesses since an important objective was to study as many elements as possible, but we have also included a few objects of relatively low surface brightness to see to what extent faint nebulae have the same properties as those of high surface brightness.

The range of ionization is from Cn 3-1, whose excitation is so low that λλ4959, 5007 are barely visible, to objects such as M1-1, whose excitation is so high that it has not been possible to calculate a satisfactory model. As has been noted since the work of Bowen and Wyse (1939) and Wyse (1942), some objects, such as NGC 2440 or NGC 6302, show a huge range in excitation—from Mg I to [Ne V], indicative of very marked inhomogeneities.

Summarizing reports on earlier phases of this investigation have been given at the 1977 Ithaca conference (Aller 1978*a*) and by Aller (1978*b*). The technique was to calculate a network of theoretical models in which the central star fluxes were those given by Cassinelli (1971). Stellar radii and nebular densities, nebular radii, and chemical compositions were treated as adjustable parameters. It was possible to represent the general level of excitation but not individual spectral line intensities for individual nebulae. The models were then used to obtain ionization correction factors (ICFs). The observational data consisted mostly of measurements made with the image-tube scanner (Aller and Czyzak 1979, hereafter AC) calibrated with photoelectric measurements. Detailed analyses were not published at that time because we wished to improve both observational data and models.

Table 1 lists the objects discussed in the present paper ordered according to right ascension. The first two columns give the common and Perek-Kohoutek (1967) catalog designations. For each nebula we list in column (4) the number of the table in which intensity data are documented. Column (5) indicates roughly whether the nebula is low (L), medium (M), or high (H) excitation. Column (6) lists the table in which details of the analysis are presented. Columns (7) and (8) give the values of the Seaton parameters:

$$t = T_\varepsilon/10{,}000,$$

and $\log x$, where

$$x = 10^{-2} N_\varepsilon/\sqrt{T_\varepsilon},$$

which are used for all elements in any nebula which is analyzed under a uniform density/temperature assumption. Such objects are indicated by a "(1)" in column (9). If two or more temperature zones are assumed, we use the designation "(2)" in column (9), or a "T," which means that a reference to notes for that particular object is indicated. Generally, we designate in columns (10) and (11) the (x, t) values for specific ions, often for N II and S II or higher ionization stages of C, N, and Ne (indicated in parentheses). The (x, t) values are chosen for interpretation of [N II] and [S II] lines from T_ε and N_ε values obtained from λ6584/λ5755 and λ6717/λ6730 ratios. For the highly ionized ions, x and t are generally adopted from theoretical models, although for [Ne IV] it is sometimes possible to use the auroral/nebular line ratios. Further discussions of these diagnostics will be found in the following sections.

Column (3) gives the interstellar extinction coefficient, C, defined as

$$C = \log F_c(\mathrm{H}\beta)/F_0(\mathrm{H}\beta),$$

where $F_c(\mathrm{H}\beta)$ is the Hβ flux corrected for interstellar extinction and $F_0(\mathrm{H}\beta)$ is the observed Hβ flux. These values of C are found usually by comparing observed and theoretical Balmer decrements. In some instances it is possible to obtain a good estimate of C by comparing *IUE* and optical data, specifically the λ1640/λ4686 ratio as suggested by Seaton (1978).

II. SELECTION OF OBSERVATIONAL DATA

Our objective was to obtain a set of homogeneous data for a number of planetary nebulae varying in excitation, structure, galactic distribution, and surface brightness. The program, described by AC, involved getting measurements with the Robinson-Wampler image-tube scanner at the Cassegrain focus of the Shane telescope at Lick Observatory. As far as possible, these data were calibrated by photoelectric photometry, using data of TPP (1977), Barker (1978*a*), and others as cited in the references, and our own measurements carried out at Mount Wilson with the 1.5 and 2.5 m telescopes.

For stellar nebulae and objects of small angular size, the calibration was straightforward. An example in point is Me 2-1 (Aller *et al.* 1981*c*). Nebulae of large angular extent offer greater difficulties. The photoelectric photometry usually covers the angular extent of the entire nebula; thus, it yields data that are to be compared directly with theoretical predictions. For an extended object, ITS data are obtained normally only in a small area. For practical reasons, the observer usually chooses the brightest portion (see, e.g., Shields *et al.* 1981), although for some objects such as NGC 6720 (Hawley and Miller 1977; Aller 1976; Barker 1980, 1982) or NGC 2452 (AC), observations may be secured at several places. The ITS enables us to measure very weak spec-

TABLE 1

LIST OF OBJECTS

Object	(PK)	C	I(ref.)	Excitation Group	Table	t	log x		t	log x	ions
NGC 40	120 + 9°1	0.65	2	L	7	0.8	- 0.8	(1)			
Hu 1 - 1	119 - 6°1	0.52	2	M	20	1.15	- 0.7	(2)	1.0	- 0.7	N II, S II
M 1 - 1	130 - 11°1	0.45	2	H	19	1.4	- 0.45	(2)	1.7	- 0.45	Ne IV, Ne V
NGC 650/651	130 - 10°1	0.43	4	M	8	1.0	- 1.25	(1)			
IC 1747	130 + 1°1	0.14	2	M	20	0.98	- 0.42	(1)			
IC 351	159 - 15°1	0.28	5	H	19	1.2	- 0.5	(1)			
IC 2003	161 - 14°1	0.17	5	H	21	1.1	- 0.18	(1)			
NGC 1535	206 - 40°1	0	2	H	21	1.09	- 0.4	(1)			
J 320	190 - 17°1	0.31	4	M	8	1.2	- 0.1	(1)			
IC 418	215 - 24°1	0.32	3	L	7	0.83	+ 0.05	(1)			
NGC 2022	196 - 10°1	0.38	5	H	25	1.37	- 0.9	(1)			
IC 2165	221 - 12°1	0.67	2	H	25	1.35	- 0.5	(2)	1.12	- 0.5	S II, N II (t = 1.5 Ne IV, 1.8 Ne V)
J 900	194 + 2°1	0.83	5	H	26	1.18	- 0.4	(2)	1.5	- 0.5	Ne IV, Ne V
NGC 2346	215 + 3°1	0.24	2	M	9	1.32	- 1.5	(1)			
NGC 2371 - 2(W)	189 + 19°1	0.29	5	H	23	1.065	- 0.8	(2)	0.93	- 0.8	N II, S II
(E)	189 + 19°1	0	5	H	23	1.24	- 1.0	(2)	0.98	- 1.0	N II, S II
NGC 2452 C	243 - 1°1	0.5	2	M	22	1.2	- 0.9	(2)	0.9	- 0.9	N II, S II (t = 1.5 Ne V)
SE						1.06	- 0.6	(2)	0.95	- 0.6	N II, S II
NE						1.03	- 0.7	(2)	0.87	- 0.7	N II, S II
NGC 3242	261 + 32°1	0	2	H	24	1.09	- 0.5	(2)	1.5	- 0.3	[Ne IV]
IC 4593	25 + 40°1	0	2	L	9	0.94	- 0.78	(1)			
NGC 6210	43 + 37°1	0	3	L	10	0.94	- 0.1	(1)			
IC 4634	0 + 12°1	0.6	3	L	10	0.95	- 0.25	(2)	1.13	- 0.2	N II, S II
NGC 6309	9 + 14°1	0.83	5	H	24	1.1	- 0.5	(2)	1.3		Ne IV, Ne V
NGC 6543	96 + 29°1	0.22	2	L	11	0.8	- 0.4	(1)			
Cn 3 - 1	38 + 12°1	0.6	2	L	11	1.01	- 0.14	(2)	0.65	- 0.12	N II, S II
IC 4776	02 - 13°1	0.05	3	L	12	0.84	- 0.1	(1)			
Hu 2 - 1	51 + 9°1	0.6	3	L	12	1.0	+ 0.3	T			
NGC 6751	29 - 5°1	0.9	2	L	13	1.0	- 1.2	(2)	0.8	- 1.0	N II, S II
IC 4846	27 - 9°1	0.45	2	L	13	0.97	- 0.05	(2	1.0	- 0.5	N II, S II
NGC 6778	34 - 6°1	0.93	3	L	14	0.8	- 0.9	(1)			
NGC 6790	37 - 6°1	1.25	2	M	14	1.13	0.0	(1)			
NGC 6803	46 - 4°1	0.6	2	L	15	0.93	- 0.05	(1)			
M 1 - 74	52 - 4°1	1.10	3	L	15	0.93	+ 0.25	(1)			
NGC 6818	25 - 17°1	0.25	2	H	26	1.25	- 0.6	T	(see text)		
NGC 6826	83 + 12°1	0.03	3	L	16	1.03	- 0.6	(1)			
NGC 6884	82 + 7°1	1.09	2	H	28	1.05	- 0.05	(2)	1.35	- 0.05	Ne IV
NGC 6905	61 - 9°1	0.09	2	H	27	1.18	- 1.05	(1)			
NGC 7026	89 + 0°1	1.20	2	M	16	0.9	- 0.10	(1)			
IC 5117	89 - 5°1	1.30	2	H	17	1.18	+ 0.5	(1)	1.45	+ 0.5	[Ne IV]
Hu 1 - 2	86 - 8°1	0.61	5	H	27	1.6	- 0.1	T	1.1	- 1	[N II], [S II], [t = 1.8, N V, Ne V]
IC 5217	100 - 5°1	0.3	2	M	17	1.1	- 0.1	(1)			
NGC 7662	106 - 17°1	0.2	5	H	28	1.3	- 0.5	(2)	1.5	- 0.5	Ne IV (t = 1.7 Ne V)
Hb 12	111 - 2°1	1.7	3	L	18	1.25	1.7	(2)	1.25	- 0.1	S II, S III, Cℓ III

TABLE 2

DATA FOR NEBULAE NOT LISTED IN TABLES 3, 4, AND 5

M 1-1	3242A (4.8), 3426A (194), 4363A (8.6), 4471 (0.75)
Hu 1-1	3727A (472), 4959A (505), 5007A (1448)
NGC 1535 ...	4026A (2.6), 4471A (5), 6584A (0.25), 6678A (2.7)
IC 2165.......	4959A (382), 5007A (1130), 6435A (0.55), 6312A (0.9)
NGC 2452 ...	6435A (0.42), (0.8), (0.72) in positions a, b, and c, respectively; 5537A (0.87), 6678A (2.1) in position c
NGC 3242 ...	3727A (8.7), 4541A (0.62), 5411A (1.7)
IC 4593.......	Czyzak, Buerger, and Aller 1975, *Ap. J.*, **198**, 431
IC 4846.......	4471A (3.57)
NGC 6790 ...	5200A (0.21), 5537A (0.18)
NGC 6803 ...	see Lee *et al.* 1974, *Ap. J.*, **192**, 159
NGC 6818 ...	6584A (35), 6678A (1.7)
NGC 6884 ...	4026A (1.9), 4471A (4.6), 4541A (0.6), 5411A (1.7), 6101A (0.18)
NGC 6905 ...	4471A (0.71), 4541A (2.3), 4686A (93), 5876A (2.7)
IC 5117.......	6435A (0.05), 7005A (0.14)
IC 5217.......	6363A (0.70), 6678A (3.1), 7325A (3.91)
NGC 40......	IC 1747, NGC 2346, NGC 6543, Cn 3-1, NGC 6751, NGC 7026; data are from AC as given, with no changes

NOTE.—The line intensities are taken from AC with the following reassessments and corrections or from other references as noted. See also references in text under individual nebula.

tral features that are not practical to observe by normal photoelectric photometry. Hence, in combining ITS and photoelectric data or, less frequently, ITS data, careful judgment often is required.

A major objective of the ITS program was to reach low levels of intensity, typically $I < 0.10$ on the scale $I(\mathrm{H}\beta) = 100$ for moderately bright objects. In this way we could obtain characteristic lines of ions such as K IV or Ca V and probe diagnostic line ratios of less abundant ions, e.g., [Ar III], $\lambda 5192/\lambda 7135$. On occasion, long dwell times were needed, even for moderately bright objects such as NGC 6741.

The AC survey was restricted to lines in the range 3700 to 8500 Å. In Table 2 we list objects for which we have employed AC intensities; other data are also used, as indicated in the notes under individual nebulae. Reassessed or corrected line intensities are indicated by "$\lambda A(I)$," e.g., $\lambda 5411$ (4.5) would mean that we now adopted 4.5 as the intensity for $\lambda 5411$ He II. Later ITS detectors sensitive to the range from 3100 to 5000 Å became available. Thus, we were able to extend measurements to the 3100–3700 Å region where previously we had only photographic results calibrated for the stronger lines by photoelectric photometry. The new measurements indicated that for the most part photographic material as recalibrated in the AC survey seemed viable.

In addition, we obtained improved ITS observations for a number of objects and data for some new objects such as IC 4776. Our procedure was to reexamine again, as necessary, the available data and define a set of "definitive" intensities which was to serve as a basis for the analysis.

Tables 3, 4, and 5 give the new set of intensities. For convenience, the objects are grouped according to excitation. References to the data for individual nebulae may be found in columns (4) and (5) in Table 1. The tabulated intensities are corrected for interstellar extinction with the Seaton (1979) $f(\lambda)$ function, which is listed in column (3) of Table 5, and with the C values of Table 1. For these objects, this material replaces and supersedes the older and less complete data in AC.

TABLE 3

ADOPTED LINE INTENSITIES IN LOW EXCITATION NEBULAE
(corrected for interstellar extinction)

		IC 418	NGC 6210	IC 4634	IC 4776	Hu 2-1	NGC MI-74	NGC 6778	NGC 6826	Hb 12
3726	[O II]	95.	30.5	36.	30.2	91.	34.	104.	12.	8.7
3729		72.	14.0						8.4	2.9
3868	[Ne III]	2.9	76.	83.6	53.4	20.	96.	60.	43.1	85.1
4026	He I		2.	2.2	1.15	2.1	2.4	3.:		2.20
4068	[S II]	2.1	1.6	0.98	2.0	1.1	5.11	3.13	0.2	2.27
4076	[S II]	0.7	0.71	0.33						
4101	H δ	24.5	28.	27.4	24.	25.2	25.2	25.7	26.7	26.5
4267	C II	0.38	0.5	0.12		0.36	0.54	0.64	0.9:	0.21
4340	H γ	47.3	46.	47.	44.	48.4	48.	46.6	46.4	45.8
4363	[O III]	0.52	6.2	5.52	3.75	2.1	6.7	1.41	5.9	21.7
4471	He I	3.47	6.:	4.64	3.76	4.35	4.57	7.86	5.3	4.81
4740	[Ar IV]		1.87	1.12	0.52		1.13		0.52	0.246
4861	H β	100.	100.	100.	100.	100.	100.	100.	100.	100.
4959	[O III]	47.	377.	317.	335.	145.	383.	161.	253.	142.
5007	[O III]	144.	1051.	893.	940.	420.	1100.	535.	770.	430.
5198 5200	[N I]	0.30			0.2	0.17		3.9		0.38
5517	[Cl III]	0.17	0.34	0.28	0.29	0.11	0.24	0.76	0.35	0.104
5537	[Cl III]	0.25	0.41	0.36	0.47	0.12[3]	0.66	0.75	0.40	0.142
5755	[N II]	2.1		0.195	0.88	1.83	1.31	3.58	0.12:	6.::
5876	He I	10.	12.7	12.1	13.0	12.8	15.5	23.	13.9	14.3
6300	[O I]	1.95		0.65	3.1	1.39	3.8	6.3		
6312	[S III]	0.65	1.0	0.88	1.63	0.38	2.22	1.94	0.31	3.9
6363	[O I]	0.60		0.23	1.0	0.45	1.09	1.89	0.31	3.9
6563	H α	272.	285.	297.	273.	282.	297.	305.	287.	285.
6584	[N II]	156.	18.	7.78	20.7	59.	35.	391.	4.5	12.
6678	He I	2.24	3.2	3.23	3.02	2.75	3.90	6.9	4.7	2.7
6717	[S II]	1.6	4.0	0.69	1.25	0.2	1.48	24.6	0.2	0.07
6730		3.6		1.34	2.56	0.5	3.16	26.8	0.3	0.116
7065	He I	4.1		5.24	9.4	6.7	10.	4.2	4.8	
7135	[Ar III]	5.4	9.5	8.91	14.0	8.	28.	14.7	5.7	
7319 7330	[O II]	20.1	4.6	2.94	13.5	24.	12.6	3.8	1.18	
7751	[Ar III]	1.1		2.14			5.8	3.7		
8583	[Cl II]	0.25								

TABLE 4

ADOPTED LINE INTENSITIES IN MEDIUM EXCITATION NEBULAE
(corrected for interstellar extinction)

		NGC 650-5	J 320
3727	[O II]	600.	
3729			21.
3868	[Ne III]	175.	125.
4026	He I	4.0	2.4
4068	[S II]	7.9	1.31
4076	[S II]	2.3	
4101	Hδ	26.3	25.6
4267	C II	0.8	0.20
4340	H γ	47.0	46.0
4363	[O III]	9.3	15.6
4471	He I	4.5	4.9
4686	He II	22.0	4.1
4740	[Ar IV]		3.9
4861	Hβ	100.	100.
4959	[O III]	376.	425.
5007	[O III]	1176.	1250.
5199	[N I]	14.	

		NGC 650-5	J 320
5517	[Cl III]		0.40
5537	[Cl III]		0.27
5755	[N II]	10.8	0.21
5876	He I	12.6	14.
6300	[O I]	39.4	0.36
6312	[S III]	3.4	0.74
6363	[O I]	13.5	0.12
6563	Hα	285.	285.
6584	[N II]	757.	8.4:
6678	He I	3.0	3.5
6717	[S II]	62.2	0.42
6730	[S II]	55.4	0.70
7065	He I		4.6
7135	[Ar III]	20.2	5.54
7319 7330	[O II]	17.3	1.24
7751	[Ar III]		1.12

TABLE 5

ADOPTED LINE INTENSITIES IN HIGH EXCITATION NEBULAE
(corrected for interstellar extinction)

		f_λ	IC 351	IC 2003	NGC 2022	J 900	NGC 2371–2372 East	NGC 2371–2372 West	NGC 6309	Hu 1 – 2	NGC 7662
3202	He II	0.426	21.0	18.2	34.4	15.8	40.2	6.7		22.7	28.
3242	[Na IV]	0.410								1.3	0.52
3345	[Ne V]	0.372		7.2	14.1	6.0	33.1	3.4	3.5:	51.4	11.0
3426	[Ne V]	0.345	4.10	3.2	39.2	16.0	98.0	13.5	11.:	153.	11.0
3726	[O II]	0.256	4.70	30.8	5.0	65.0	55.5	183.	8.7	60.5	6.45
3729	[O II]		2.30		4.6				4.9		3.65
3868	[Ne III]	0.207	96.1	77.8	57.4	92.0	90.5	130.	97.7	91.3	89.
4026	He I	0.194	1.4	1.5		2.1	1.9	1.5	1.88	1.8	1.2
4068	[S II]	0.185	1.1	0.76		2.4	1.9	4.7	2.8	3.56	0.69
4076	[S II]	0.183	0.25	0.56		0.6				1.23	0.26
4101	H δ	0.177	25.6	25.7	26.0	25.4	25.8	25.1	29.	25.6	25.7
4187	C III	0.157		0.19	0.50	0.43				0.08	0.4
4200	He II	0.154		0.65	2.1	0.61	1.6	1.1	1.48	1.0	1.3
4267	C II	0.139	0.43	0.44	0.90	0.83		0.92	0.64	0.30	0.62
4340	H γ	0.121	47.8	47.1	45.6	47.0	46.9	48.2	47.0	45.9	45.9
4363	[O III]	0.116	14.1	11.5	11.6	12.6	15.0	13.5	11.5	19.8	16.8
4471	He I	0.090	2.3	3.1	0.46	3.0	2.0	3.6	2.46	3.8	2.8
4541	He II	0.074		1.8	3.1	1.5	4.3	2.3	2.53	3.18	2.42
4647	C III	0.049	0.88	0.82	1.63	0.80			0.9:		0.53
4650	C III	0.048									0.31
4658	C IV	0.046			0.81	0.68			0.7	0.5	0.32
4686	He II	0.040	51	38.0	108.	46.0	106.	59.6	68.	88.3	69.3
4725	[Ne IV]	0.031	0.32	0.34	2.12	0.63	3.1	2.3	0.47	1.77	0.8
4740	[AR IV]	0.028	6.5	3.4	11.0	2.3	13.2	6.0	7.64	5.8	6.8
4861	H β	0	100.	100.	100.	100.	100.	100.	100.	100.	100.
4922	He I	-0.014		0.84		0.6			0.9:	0.24	0.5
4959	[O III]	-0.022	378.	350.	230.	342.	380.	508.	411.	267.	366.
5007	[O III]	-0.033	1209.	1130.	683.	1100.	1150.	1615.	1220.	772.	1088.
5191	[Ar III]	-0.072		0.10						0.26	0.10
5200	[N I]	-0.074		1.2		0.28		1.9		2.5	0.11
5309	[Ca V]	-0.097			0.11					0.19	0.04:
5323	[Cℓ IV]	-0.100		0.04	0.11				0.07[4]	0.03:	0.013
5411	He II	-0.118	3.9	2.7	7.0	3.1	7.9	3.8	5.28	6.73	4.86
5517	[Cℓ III]	-0.140	0.14	0.38	0.43	0.23	1.2	1.2	0.44[5]	0.38	0.37
5537	[Cℓ III]		0.14	0.46	0.37	0.28	1.1	1.2	0.63	0.55	0.43
5755	[N II]	-0.183	1.0	1.0		0.72	0.80	2.4	0.20	4.8	0.084
5801	C IV	-0.192		0.42:		0.37				0.2	0.17
5812	C IV			0.21:						0.2	0.16
5876	He I	-0.205	6.0	9.1	2.0	8.3	4.0	8.3	8.58	10.0	7.58
6101	[K IV]	-0.243	0.20	0.20	0.57				0.36[5]	0.28	0.36
6300	[O I]	-0.275				4.5	4.6	8.9		6.25	
6312*	[S III]	-0.277	0.46	1.1	1.84	1.0	5.4	4.6	1.50	2.95	1.3
6363	[O III]	-0.285		1.0		1.6	1.4	2.6		1.94	
6435	[Ar V]	-0.296	0.22		1.2	0.14	2.7	0.85	1.1:	1.10	0.34
6563	Hα	-0.315	286.	287.	288.	285.	296.	298.	286.	285.	287.
6583	[N II]	-0.317	0.50	31.		35.4	51.1	187.	12.	184.	5.12
6678	He I	-0.331	1.9		0.84	2.0	1.3	2.9	1.41	2.92	2.24
6716	[S II]	-0.336	0.10	1.6	0.48	1.7	8.6	22.	1.34	4.85	0.39
6730	[S II]	-0.338	0.14	3.0	0.63	2.8	9.5	27.2	2.26	8.85	0.60
7005	[Ar V]	-0.375	1.0:	0.31	2.5	0.39	4.4	1.2	3.2	2.37	0.58
7135	[Ar III]	-0.391	6.0	8.7	8.9	5.4	22.1	26.0	13.3	10.5	9.45
7319	[O II]	-0.413	1.1:		0.87	4.1		6.1	2.41	12.6	1.40
7330	[O II]					3.7					
7530	[Cℓ IV]	-0.436			1.20				0.47	0.25	0.46
7751	[Ar III]	-0.460				1.2	5.3	7.1	2.80	2.41	2.39
8045	[Cℓ IV]	-0.489			3.1	0.44			0.81	0.86	0.97
8577	[Cℓ II]	-0.535								0.36	

*Blend with 6310 He II.

We can estimate accidental errors from the internal consistency of the individual measurements. These depend not only on the strength of the line but also on the nebular surface brightness. For nebulae of moderately high surface brightness, the strongest lines should be accurate to 5%–8%. The errors will increase to 10%–20% for lines of intensity in the neighborhood of 2 to 10 [on the scale $I(\mathrm{H}\beta)=100$], and 25%–35% for lines of intensity of ~ 1.0. The intensities of yet weaker lines may be in error by a factor of 2. Errors are naturally larger for objects of low surface brightness and near the extreme ends of the spectral range.

Systematic wavelength-dependent effects can arise from errors in the energy distributions of the comparison stars that are used to establish the response function, from the choice of the extinction (which may be produced by interstellar dust and dust within the nebula itself), and from errors in the atmospheric extinction. For comparing lines in the 3700 Å region with lines in the 7500 Å, we suspect that errors of the order of 10% may arise typically from these causes. Larger errors may accrue in comparing lines in the 3200–3400 Å region with those in the 7500 Å region. Among popular diagnostics of nebular plasmas, the λ3727/λ7325 [O II] ratio is particularly sensitive to wavelength-dependent errors.

An even more troublesome annoyance can rise from spatially small-scale line intensity variations from point to point in a nebula. An example is provided by NGC 7009 where a long coudé slit placed in the bright inner ring parallel to the major axis gave $I(\lambda 3727)$ [O II] = 11.2, while the short 2″×2″ ITS slot gave $I(\lambda 3727)=6.0$. The discordance is not due to inadequacies of the photographic photometry used at the coudé, but rather to the fact that the longer coudé slit extended into regions of lower excitation and higher [O II] intensity. The consequence for a nitrogen abundance determination in the bright ring is that using the popular $n(\mathrm{N})/n(\mathrm{N\ II})=n(\mathrm{O})/n(\mathrm{O\ II})$ approximation, $n(\mathrm{N})/n(\mathrm{H})$ is now found to be 7.5×10^{-5} instead of 4×10^{-5} in the high excitation region along the minor axis of the nebula, as compared with a value of 1.17×10^{-4} in the low excitation region at the end of the major axis (Czyzak and Aller 1979). In some instances, it must be recognized that the only data available pertain to a bright ring, a bright central region, or a typical region in the disk (Aller and Epps 1976, AC).

We have also included *IUE* data from published sources. For nebulae of small angular size, there is no particular problem. Both the photoelectric measurements and the *IUE* measurements with the elliptical slot cover the entire nebula. In objects of high excitation, the λ1640/λ4686 ratio is a known function of the temperature (Seaton 1978). If the temperature, T_ε, is known, we can compare observed and predicted ratios to assess the extinction.

In objects of appreciable size, the elliptical slot of the *IUE* does not cover the same region as is observed with the ITS or by photoelectric photometry. If isophotic contours are available, it is possible to overcome this difficulty as Harrington *et al.* (1982) have illustrated for NGC 7662. Generally, when contours are not known and the *IUE* slot covers only a portion of the nebula, the extinction must be estimated from other sources. Then one may refer all intensities to λ1640, which in turn may be linked to λ4686 and eventually to Hβ. The procedure is described by Shields *et al.* (1981).

A more serious difficulty pertaining to *IUE* intensities is that they may be "contaminated" by contributions from the central star. In many of the early published investigations, the observers centered on a bright central star, and it is impossible to separate nebular and stellar contributions for many lines.

III. COMMENTS ON THEORETICAL MODELS

For faint and distant objects, it is practical to obtain diagnostics from only a small number of ions, typically (λ5007 + λ4959)/λ4363 [O III], λ6584/λ5755 [N II], and λ6717/λ6730 [S II] (see, e.g., Barker 1978*b*). Then one calculates $N(X_i)$ for each observed ion and derives the ionization correction factors with the aid of extrapolation procedures such as those employed by Peimbert and Costero (1969). The principle involved is not greatly different from that suggested by Bowen and Wyse (1939).

The other extreme is a multidensity model arranged to reproduce the line intensities of a well-observed nebula such as NGC 7662 in detail (see Harrington *et al.* 1982). This procedure is painstaking, difficult, and expensive, and although it works for a symmetrical object, it cannot be expected to do as well for complex structures such as NGC 2440, 6302, or 7027. Indeed, for the latter object, it may be necessary to invoke a time-dependent model (Shields 1978*a*).

Our procedure occupies a middle ground (see Shields *et al.* 1981). We use theoretical models as interpolation devices to obtain ionization correction factors which are then applied to ionic concentration, $N(X_i)$, to get the total abundance $N(X)$. The argument is that if it is possible to find a model that represents the general level of excitation, certain excitation-sensitive line ratios, and the intensities of most of the principal lines as well, then such a model gives better ICFs than empirical formulae. Ad hoc formulae cannot take into account essential physical processes such as charge exchange, the effect of a changing radiation field through the nebula, and differing absorptivities of ions for continuum radiation. Physical models have their limitations, of course. They involve unrealistic assumptions about symmetry and density fluctuations, or the lack thereof. Among the most severe difficulties, of course, are those imposed by condensations and partially ionized clouds in high excitation objects. In the end, we emphasize that there is no substitute for observing as many elements in as many stages of ionization as is possible. This means extending our observed range to the ultraviolet and to the infrared and getting to as faint lines as is possible.

The first attempts (Aller 1978*a*, *b*) were to construct networks of uniform density models based on energy distributions by Cassinelli (1971) or Hummer and Mihalas (1970). The procedures are described in detail by Keyes and Aller (1978, 1980). For many nebulae, the restrictions are too severe to permit a detailed representation of the line intensities. Furthermore, at that time, no *IUE* data were available. The abundance of carbon, for example, depended on weak permitted lines of C II, C III, and C IV interpreted as recombination features. The nitrogen abundance required extrapolations from N(N II)/N(H II) ratios, a step which is often inaccurate in models of objects of medium to high excitation.

In the present analysis we have used models tailored for individual nebulae as far as possible (Aller 1982). The original program, due to Balick (1975), was metamorphosed to include additional ions, important physical processes such as charge exchange and dielectronic recombination, and improved atomic data such as continuous absorptivities, recombination coefficients, A values, and collisional cross sections. It still includes some simplifications such as the on-the-spot approximation in the treatment of radiative transfer.

As excitation parameters we chose λ5876/λ4686, He I/He II, λ3727/(λ5007+λ4959) [O II]/[O III], and λ3868/λ3426 [Ne III]/[Ne V]. We tried to represent these ratios by adjusting $N_{\rm H}$, the cutoff radius of the nebula, r_c, the energy distribution from the central star, $F_\nu(x)$, and the chemical composition. Modifications of the radius of the central star have minor effects on the pattern of excitation and negligible effects on the finally derived abundances. The procedures are described in detail elsewhere (Aller *et al.* 1981*a*, *b*, *c*; see also Osterbrock 1974). Values for atomic parameters are taken mostly from the paper by Shields *et al.* (1981).

The models differ from those of Köppen and his associates (Köppen 1979; Köppen and Tarafdar 1978; Che and Köppen 1981) largely in that they have postulated Planckian stellar energy flux distributions, the temperatures for which are determined by the He II/Hβ ratio. On the other hand, we have often modified the UV fluxes mentioned above, although on some occasions the initial Cassinelli or Hummer and Mihalas energy distributions would work well.

Although most of the lines in the optical region can be well represented, difficulties are often encountered with ions of the $3p^3$ configuration such as those of [S II], [S III], [Cl III], [Cl IV], [Ar III], [Ar IV], and [Ar V]. Some of the trouble may arise from effects of partially ionized blobs, and some may arise from inadequacies in the A values and collisional cross sections (Czyzak *et al.* 1980).

Less success is encountered in the ultraviolet region (Aller *et al.* 1981*b*). Models that handle the optical region will tend to show discordances. For example, the C IV λ1550 pair tends to be systematically weaker than predicted by the models. Harrington *et al.* (1982) have attributed this weakness to repeated scattering of and absorption of C IV quanta by dust grains in the nebula. The published intensities of emission lines in the *IUE* region often refer to nebula plus star. In nebulae of large angular size, one can avoid the central star, but for those of small angular size, emission lines of stellar origin, e.g., N V λ1240, inevitably become confused with emission lines arising in the nebula itself. As improved *IUE* data on stars and nebulae separately become available, it will be possible to refine the analyses.

For a number of nebulae, specific models were not calculated. In some instances we found that standard nebular models with Cassinelli central star fluxes would yield adequate results. In other instances, e.g., Hu 1-2, complexities imposed by stratification and filamentary structure combined with a high excitation did not permit a good representation by any reasonable model. The best we could do was to construct a model that would give the right level of excitation and use this to estimate ICFs. It must be admitted, however, that the best chance here is to cover as many stages of ionization as possible, so that the influence of inaccuracies in the ICFs will be minimized.

IV. DERIVATION OF ICF FACTORS AND ABUNDANCES

Given the adopted line intensities, corrected for interstellar extinction (Tables 2 through 6), the first step is to construct appropriate diagnostic diagrams, using principally the well-known ratios of

[λ4959+λ5007]/λ4363	[O III],
λ3729/λ3726	[O II],
λ3727/λ7325	[O II],
λ6717/λ6730	[S II],
λ6583/λ5755	[N II],
λ5517/λ5537	[Cl III].

Additional diagnostic criteria that may be used in determinations of (x, t) are listed in AC, Table VIII. Some of these are available for well-observed objects, e.g., NGC 7662. Figures 1 through 12 show typical diagnostic diagrams. Auroral/nebular line ratios in p^2 configurations ([N II],[O III],[Ar III],[S III]) are used principally to determine T_ε, while ratios of nebular-type lines in p^3 configurations depend on both N_ε and T_ε.

TABLE 6

ADOPTED VALUES OF ULTRAVIOLET REGION INTENSITIES CORRECTED FOR INTERSTELLAR EXTINCTION AND NORMALIZED TO $I(H\beta) = 100$

		(1) NGC 1535	(1) J 320	(2) NGC 2022	(1.2) J 900	(1) IC 2165	(1) NGC 3242	(1) NGC 6818	(1) Hu 1 - 2	(3) NGC 7662
1239/1241	N V	250*			103	41		13.6	193	---
	Si IV									
1398/1403	O IV]	29		92	43	46		37.5	81.0	32
1487	N IV]		31	68	105	50		51.1	245	34
			20							
1548/1550	C IV	91	382	837	998	1010		158	671	536
			196							
1640	He II	121		724	284	287	154	479	626	294
1661/1666	O III]				40	26		38.7		19
1747	N III]	66				26		21.7	167	9.5
1892	Si III		14.3		217			15.2		
			7.31							
1906/1909	C III]	70	558	429	1639	1345	127	827	521	304
			286							
2328	C II], [O III]				286	81		52	71	12.3
2422	[Ne IV]		36	271	97	113	11.9	182	248	95
2284	[Mg V]					7.61		8.3		
2801	Mg II							1.72		
Assumed C		0	0.31	0.38	0.83	0.67	0	0.25	0.76	0.2
Ext. Coeff.			0.16							

NOTES.—IC 4846, assuming $C = 0.45$; we find $I = 35.9$ for C III λ1908. For J320 we have assumed two different values of the extinction coefficient: hence, there are two sets of derived intensities.

REFERENCES.—(1) Boggess, Feibelman, and McCracken 1981. (2) Carpenter and Czyzak 1982. (3) Harrington and Lutz 1979.

Ideally, of course, all the lines in a diagnostic diagram should intersect at a point. The fact that they do not is usually interpreted as meaning that different radiating zones have different electron temperatures and densities, but this may not be the complete story. Part of the scatter certainly arises from observational errors; for example, for this reason we cannot place much trust in T_ε values obtained from the λ5192/λ7135 ratio in [Ar III]. Yet some of the scatter must arise from inadequacies in atomic parameters, A values, and collision strengths.

In most instances, we have been able to select a single (x, t) combination to represent the temperature and density combination appropriate for a particular nebula. Nevertheless, for some objects there appear to be definite differences in T_ε values for [N II] and [O III] zones (see Table 1). Such temperature differences between N II and O III zones have been found by many workers (see, e.g., Barker 1978*a*), but they have not been predicted quantitatively by theory. Shields *et al.* (1981) regard this discordance as one of the greatest shortcomings of theoretical models. For highly ionized species represented by one or two ions, though, we have to rely on these models.

Once the diagnostics are chosen, we may calculate the ratio $N(X_i)/N(\text{H II})$ from the observed line intensities

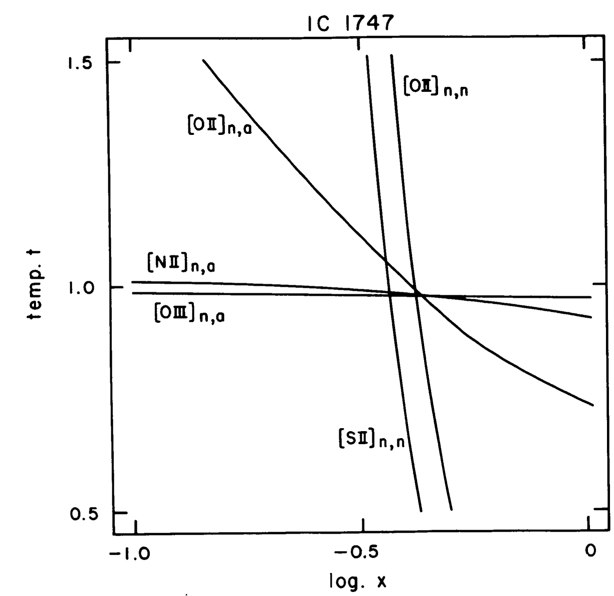

FIG. 1.—Diagnostic diagram for IC 1747. For each diagnostic we plot the temperature parameter, $t = 10^{-4}\ T_\varepsilon$, against $\log x$, where Seaton's parameter $x = 0.01\ N_\varepsilon/\sqrt{T_\varepsilon} = 10^{-4}\ N_\varepsilon/\sqrt{t}$. The subscripts (n, a) and (n, n) indicate the type of ratio involved. Thus, (n, n) refers to the ratio of two nebular-type transitions, e.g., λ6717/λ6730 [S II] and λ3726/λ3729 [O II]. Similarly, (n, a) refers to the ratio of nebular to auroral-type transitions, e.g., λ6584/λ5755 [N II] or (λ5007 + λ4959)/λ4363 [O III].

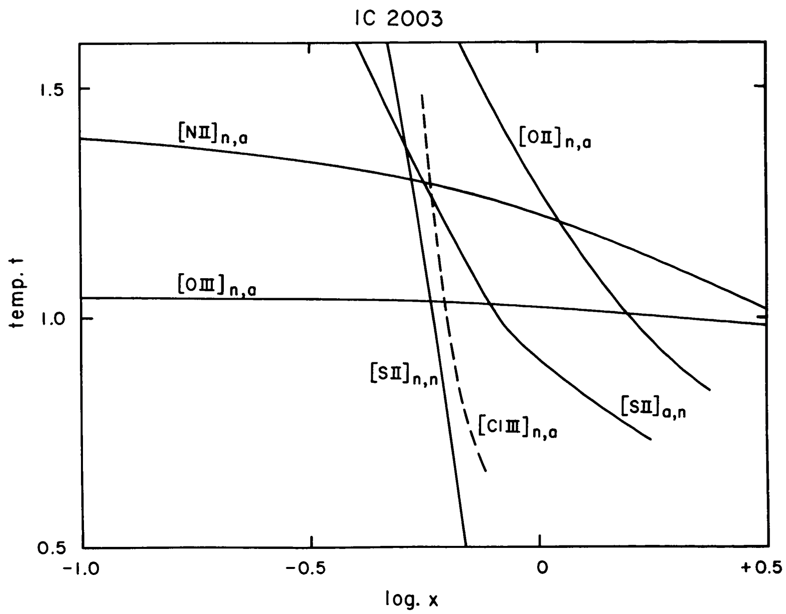

FIG. 2.—Diagnostic diagram for IC 2003. The ratio of the two nebular transitions of [Cl III], indicated by the dotted line, gives an uncertain estimate of $\log x$, because of weakness of the lines and uncertainties in the atomic parameters. Notation is as in Fig. 1.

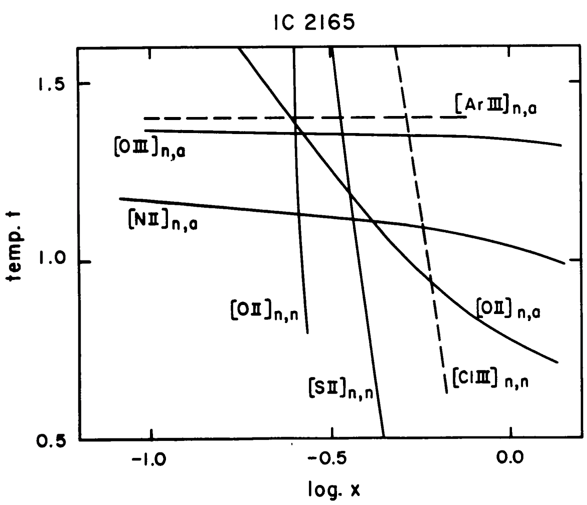

FIG. 3

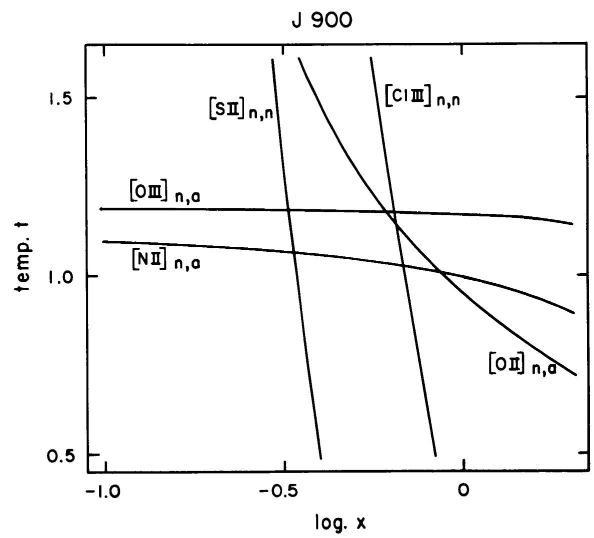

FIG. 4

FIG. 3.—Diagnostic diagram for IC 2165. Here the ratio of the nebular to auroral transitions in [Ar III] is uncertain because of the weakness of the auroral-type λ5192 transition. We indicate by dotted lines those diagnostics that are uncertain largely because of the weakness of the observed transitions.

FIG. 4.—Diagnostic diagram for J 900. For notation see Fig. 1.

by well-known expressions (see col. [3] of Tables 7–28 for wavelengths of lines used in calculating the ionic concentrations). Necessary atomic parameters are listed by Shields *et al.* (1981) or in the references cited therein. We then form the sum $\Sigma N(X_i)$ over all observed stages; in some fortunate instances this is the same as the total atomic abundance. Note that each ionic concentration in Tables 7–28 is given in terms of hydrogen ions, N(H II). Since hydrogen is all ionized in the radiating zone, $N(X_i)/N(\text{H II}) = N(X_i)/N_{\text{H}}$.

The ICFs must be taken from the individual theoretical models. Then $N(X) = (\text{ICF}) \times \Sigma N(X_i)$. Where special theoretical models are available, we tabulate also the model predictions for abundances for the nebula in question. These often differ from the "derived" or $N(X)$ values. Typically, $\Delta \log N \approx 0.1$, although larger discor-

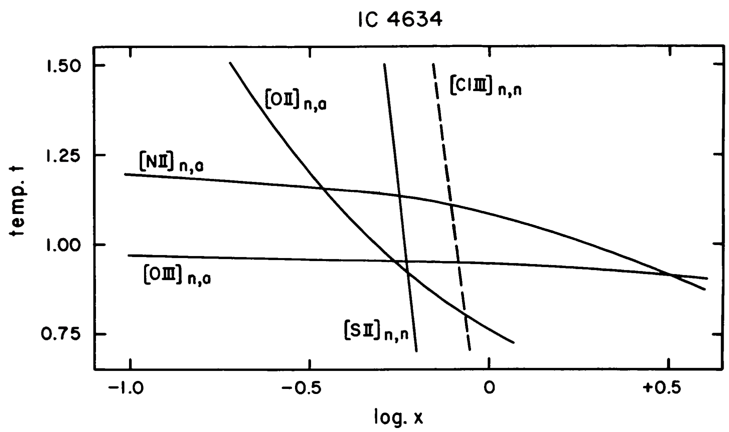

FIG. 5

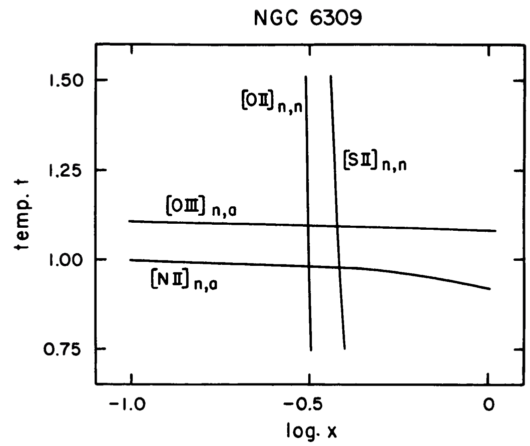

FIG. 6

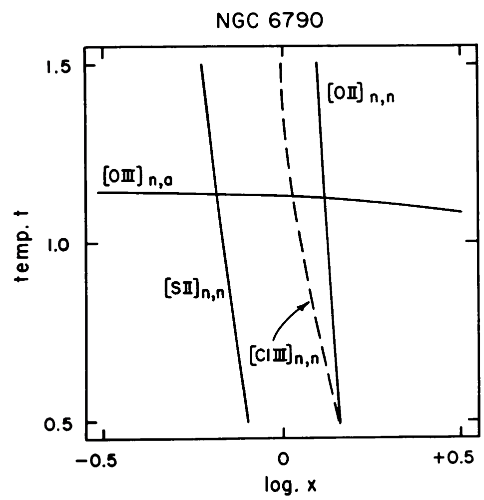

FIG. 7

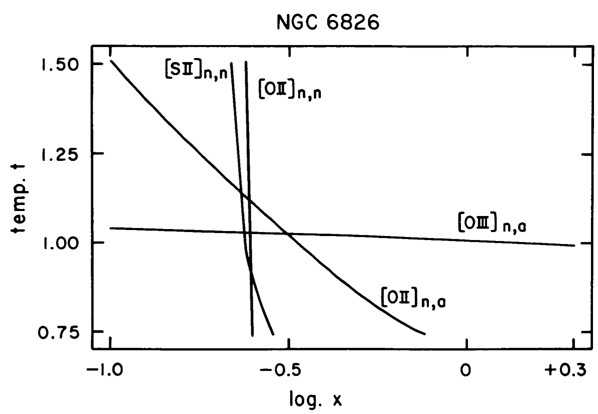

FIG. 8

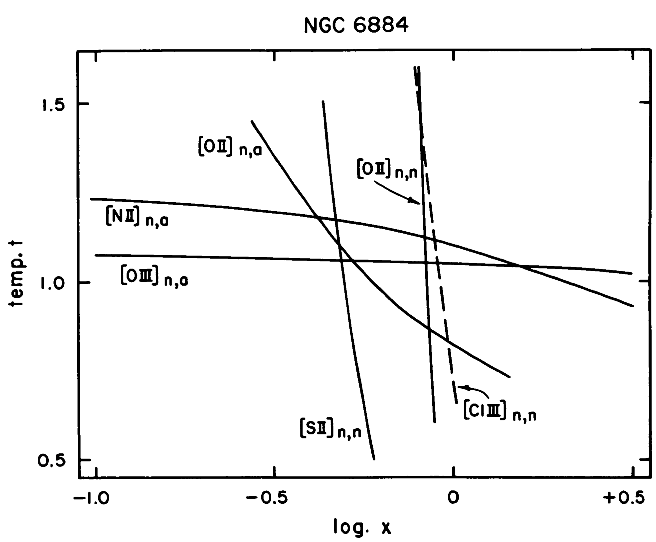

FIG. 9

FIG. 5.—Diagnostic diagram for IC 4634. For notation see Fig. 1.
FIG. 6.—Diagnostic diagram for NGC 6309. This diagram is drawn for the central region; for notation see Fig. 1.
FIG. 7.—Diagnostic diagram for NGC 6790. For notation see Fig. 1. Again, the [Cl III] diagnostic is uncertain.
FIG. 8.—Diagnostic diagram for NGC 6826. For notation see Fig. 1.
FIG. 9.—Diagnostic diagram for NGC 6884. For notation see Fig. 1.

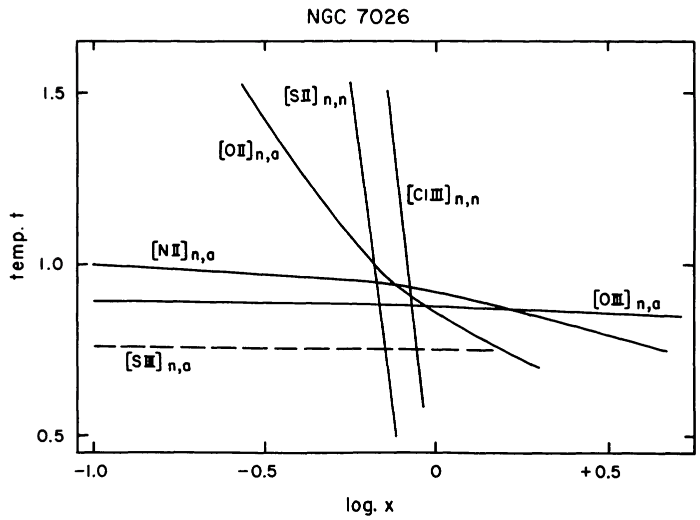

FIG. 10

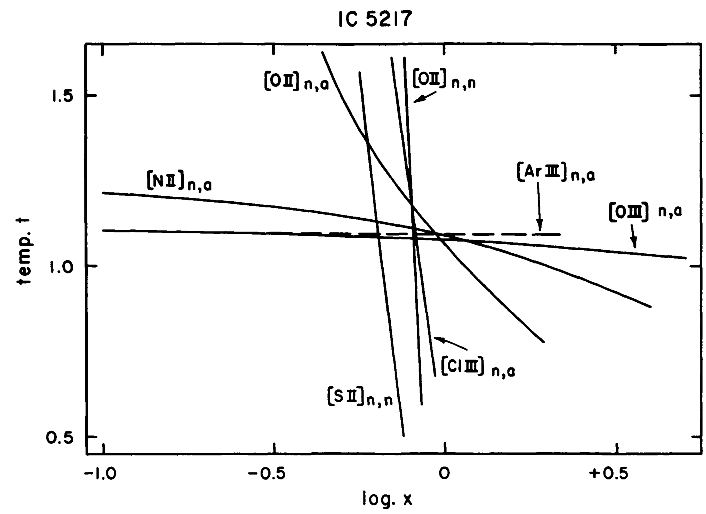

FIG. 11

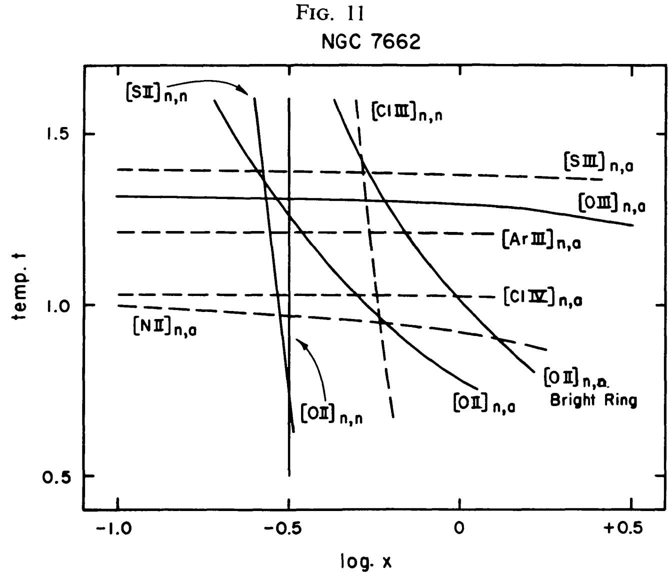

FIG. 12

FIG. 10.—Diagnostic diagram for NGC 7026. The [S III] nebular to auroral line ratio is uncertain. For notation see Fig. 1.

FIG. 11.—Diagnostic diagram for IC 5217. For notation see Fig. 1; the [Ar III]$_{n,a}$ diagnostic is uncertain.

FIG. 12.—Diagnostic diagram for NGC 7662. Although there are a large number of diagnostics available for this bright nebula, many of them are uncertain, as indicated by dotted lines. The [O II]$_{n,a}$ diagnostics are given for both total nebular emission using Peimbert's data and for a point the bright ring of presumably higher density.

1983ApJS...51..211A

TABLE 7

IONIC CONCENTRATIONS, IONIZATION CORRECTION FACTORS, ABUNDANCES DERIVED FROM MODELS

		IC 418 $N(X_i)$	$\Sigma N(X_i)$	ICF	$N(X)$	Model	NGC 40 $N(X_i)$	$\Sigma N(X_i)$	ICF	Abundance
He I		0.070		1.32	0.093	0.12	0.05			>0.5 (-1)
C III	4267 1909	4.04 (-4)	4.04 (-4)	1.53	6.2 (-4)†	6.0 (-4)				
N II	6584	5.91 (-5)	5.91 (-5)	1.24	7.3 (-5)	6.0 (-5)	9.61 (-5)	9.61 (-5)	1.02	9.8 (-5)
O II	3727	3.39 (-4)	4.36 (-4)	1.00	4.36 (-4)	4.25 (-4)	5.92 (-4)	6.01 (-4)	1.0	6.0 (-4)
O III	4959/5007	0.969(-4)					9.3 (-6)			
Ne II	12.8 μ	6.8 (-5)	7.44 (-5)	1.0	7.44 (-5)	4.0 (-5)				
Ne III	3868	0.64 (-5)								
S II	6717/6730	0.23 (-6)	3.88 (-6)	1.06	4.11 (-6)	4.2 (-6)	0.99 (-6)	4.05 (-6)	1.0	4.09 (-6)
S III	6312	3.55 (-6)					3.06 (-6)			
S III	9069	3.72 (-6)								
Cl II	8583	2.80 (-8)	8.24 (-8)	1.06	8.73 (-8)	1.4 (-7):				
Cl III	5537	5.44 (-8)					1.01 (-7)			>1.0 (-7)
Ar II	7 μ	1.43 (-6)	2.08 (-6)	1.11	2.31 (-6)	4.6 (-6)	6.17 (-7)			>6.2 (-7)
Ar III	7135	0.65 (-6)								

†In this and subsequent tables, a (†) means that the carbon abundance is based on λ4267.

TABLE 8

IONIC CONCENTRATIONS, IONIZATION CORRECTION FACTORS, ABUNDANCES DERIVED FROM MODELS

		J320 $N(X_i)$	$\Sigma N(X_i)$	ICF	Abundance	NGC 650–651 $N(X_i)$	$\Sigma N(X_i)$	ICF	Abundance
He I		0.103	0.107		0.107	0.086	0.106	1.0	0.106
He II		0.004				0.020			
C III	4267	2.24 (-4)	2.24 (-4)	1.95	4.4 (-4)†	1.03 (-3)	1.03 (-3)	1.2	1.2 (-3)†
N II	6584	1.06 (-6)	1.06 (-6)	35.7	3.8 (-5)	1.45 (-4)	1.45 (-4)	2.5	3.6 (-4)
O II	3727	5.34 (-6)	2.37 (-4)	1.07	2.54(-4)	2.50 (-4)	6.3 (-4)	1.1	6.9 (-4)
O III	4959/5007	2.32 (-4)				3.80 (-4)			
Ne III	3868	6.15 (-5)	6.15 (-5)	1.09	6.7 (-5)	1.70 (-4)	1.7 (-4)	2.06:	3.5 (-4)
S II	6717/6730	1.89 (-8)	8.82 (-7)	6.2	5.47(-6)	2.51 (-6)	1.08 (-5)	1.7	1.83 (-5)
S III	6312	8.63 (-7)				8.27 (-6)			
Cl III	5537	1.863(-8)	1.863(-8)	1.8	3.35(-8)				
Ar III	7135	2.98 (-7)	1.33 (-6)	1.03	1.37(-6)	1.60 (-6)		2.0:	3.2 (-6):
Ar IV	4740	1.03 (-6)							

TABLE 9

IONIC CONCENTRATIONS, IONIZATION CORRECTION FACTORS, ABUNDANCES DERIVED FROM MODELS

		NGC 2346 $N(X_i)$	$\Sigma N(X_i)$	ICF	Abundance	IC 4593 $N(X_i)$	$\Sigma N(X_i)$	ICF	Abundance $N(X)$	Model
He I		0.115	0.133	1.0	0.133	0.130	0.130	1.0	0.130	0.16
He II		0.018								
N II	6584	3.27 (-5)	3.27 (-5)	3.5	1.15 (-4)	2.47 (-6)	2.47 (-6)	5.15	1.27 (-5)	1.0 (-5)
O II	3727	5.012(-5)				5.0 (-5)				
O III	4959/5007	1.35 (-4)	1.85 (-4)	1.17	2.16 (-4)	2.18 (-4)	2.68 (-4)	1.0	2.68 (-4)	2.5 (-4)
Ne III	3868	3.09 (-5)	3.09 (-5)	1.5	4.64 (-5)	3.26 (-5)	3.26 (-5)	1.03	3.36 (-5)	6.3 (-5)
S II	6717/6730	1.39 (-7)		11	1.5 (-6):	8.07 (-8)				
S III	6312					3.09 (-6)	5.90 (-6)	1.0	5.9 (-6)	4.0 (-6)
	10.6 μ					2.80 (-6)				
Ar III	7135	1.19 (-6)		2.93	3.5 (-6)	6.6 (-7)	6.6 (-7)	1.41	9.3 (-7)	1.0 (-6)

TABLE 10

IONIC CONCENTRATIONS, IONIZATION CORRECTION FACTORS, ABUNDANCES DERIVED FROM MODELS

		NGC 6210				IC 4634			
		$N(X_i)$	$\Sigma N(X_i)$	ICF	Abundance	$N(X_i)$	$\Sigma N(X_i)$	ICF	Abundance
He I		0.102	0.102	1.0	0.102	0.088	0.088	1.0	0.088
C III	4267					1.30 (-4)	1.30 (-4)	1.04	1.35 (-4)†
N II	6584	4.6 (-6)	4.6 (-6)	10.5	4.83 (-5)	1.19 (-6)	1.19 (-6)	1.05	1.25 (-5)
O II	3727	4.55(-5)	5.01 (-4)	1.0	5.01 (-4)	3.33 (-5)	4.03 (-4)	1.0	4.03 (-4)
O III	4959/5007	4.56(-4)				3.70 (-4)			
Ne III	3868	9.62(-5)	9.62 (-5)	1.0	9.62 (-5)	1.00 (-4)	1.00 (-4)	1.0	1.01 (-4)
S II	6717/6730	1.63(-7)				5.18 (-8)			
S III	6312	3.14(-6)	2.13 (-5)	1.0	2.13 (-5)	2.55 (-6)			
S III	9069	3.37(-6)							
S IV	10.5 μm	1.78(-5)							
Cℓ III	5537	6.57(-8)	6.57 (-8)	1.5	9.9 (-8)	5.69 (-8)	5.69 (-8)	1.61	9.16 (-8)
Ar III	9.0 μm	2.9 (-6)	4.0 (-6)		4.0 (-6)	7.99 (-7)	1.41 (-6)	1.0	1.41 (-6)
	7135	[0.88(-6)]		1.0	or				
Ar IV	4740	1.06(-6)	[1.94 (-6)]		[1.94 (-6)]	6.11 (-7)			

In NGC 6210, two argon abundance estimates are given, one based on the infrared measurements by Beck et al. (1981) and the other, in [ ], based on optical data.

TABLE 11

IONIC CONCENTRATIONS, IONIZATION CORRECTION FACTORS, ABUNDANCES DERIVED FROM MODELS

		Cn 3 - 1					NGC 6543				
		$N(X_i)$	$\Sigma N(X_i)$	ICF	Abundance N(X)	Model	$N(X_i)$	$\Sigma N(X_i)$	ICF	Abundance N(X)	Model
He I							0.111	0.111	1.0	0.111	0.115
C III	4267	3.3 (-4)	3.3 (-4)	1.6	5.3 (-4)	5.0 (-4)	7.04(-4)	7.04(-4)	1.78	1.25 (-3)	
N II	6583	1.68(-4)	1.68(-4)	1.1	1.85(-4)	4.9 (-5)	6.15(-6)	6.15(-6)	14.1	8.67 (-5)	8.0 (-5)
O II	3727	1.55(-4)	1.61(-4)	1.04	1.68(-4)	1.3 (-4)	3.61(-5)	5.58(-4)	1.0	5.58 (-4)	4.80(-4)
O III	4959/5007	5.7 (-6)					5.22(-4)				
Ne III	3868	4.23(-7)	4.23(-7)	143	6.05(-5)	8.5 (-5)	1.37(-4)	1.37(-4)	1.03	1.41 (-4)	1.40(-4)
S II	6717/6730	1.44(-6)	2.49(-6)	1.0	2.5 (-6)	2.5 (-5)	8.19				
S III	6312	1.05(-6)					4.8 (-6)	6.46(-6)	1.58	1.02 (-5)	8.0 (-6)
	9069						9.0 (-6)				
Cℓ III	5537	4.19(-8)	4.19(-8)	6	2.5 (-7)	1.25(-7)	1.32(-7)	1.32(-7)	2.24	2.96 (-7)	2.20(-7)
Ar III	7135						1.93(-6)	2.65(-6)	1.0	2.65 (-6)	4.50(-6)
Ar IV	4740						7.23(-7)				

dances tend to occur for N and S. The N discordance occurs because in most instances an attempt was made to fit the [N II] λ6584 line with the model, rather than the UV lines. It illustrates a difficulty frequently encountered in trying to fit ions at the extreme ends of the ionization range. In some complex, high-excitation objects, such as NGC 2371–2, the assumption N(N)/N(N II) = N(O)/N(O II) may work better than theoretical models.

The sulfur discrepancy arises from the fact that most models cannot be made to fit both [S II] and [S III] simultaneously. In most instances n(S III) ≫ n(S II). Abundances of Ne, Ar, and S in some of our listed nebulae, viz., IC 418, IC 2165, NGC 3242, IC 4593, NGC 6210, NGC 6790, NGC 6803, NGC 6884, NGC 7026, IC 5117, IC 5217, and NGC 7662, have already been discussed by Beck *et al.* (1981) with the aid of these models. For completeness, we include their (sometimes slightly modified) results for Ne, S, and Ar for these objects in our tabulation. When lines of [S II], [S III], and [S IV] are all observed, the sulfur abundance should be well established. Barker (1978*c*) and Dinerstein (1980)

TABLE 12

IONIC CONCENTRATIONS, IONIZATION CORRECTION FACTORS, ABUNDANCES DERIVED FROM MODELS

		IC 4776				Hu 2-1							
		$N(X_i)$	$\Sigma N(X_i)$	ICF	Abundance	$N(X_i)$	$\Sigma N(X_i)$	ICF	$N(X)_I$	Model	$N(X_i)$*	$\Sigma N(X_i)$*	$N(X)_{II}$*
He I		0.086	0.086	1.0	0.086	0.093	0.093	1.0	0.093	0.088	0.089	0.089	0.089
C III	4267					3.92 (-4)	3.92 (-4)	1.10	4.31 (-4)†		3.85 (-4)	3.85 (-4)	4.22 (-4)†
N II	6584	7.3 (-6)	7.3 (-6)	10.5	7.80 (-5)	1.16 (-5)	1.16 (-5)	3.44	4.0 (-5)	4.1 (-5)	7.44 (-6)	7.44 (-6)	2.56 (-5)
O II	3727	5.6 (-5)	6.67(-4)	1.0	6.67 (-4)	1.59 (-4)	2.99 (-4)	1.0	3.0 (-4)	2.3 (-4)	2.54 (-4)	4.72 (-4)	4.72 (-4)
O III	4949/5007	6.11(-4)				1.40 (-4)					2.18 (-4)		
Ne III	3868	1.12(-4)	1.12(-4)	1.0	1.12 (-4)	1.94 (-5)	1.94 (-5)	1.0	1.94 (-5)	3.0 (-5)	3.03 (-5)	3.03 (-5)	3.03 (-5)
S II	6717/6730	2.13(-7)	8.6 (-6)	1.54	1.32 (-5)	3.46 (-8)	9.48 (-7)	1.28	1.21 (-6)	2.0 (-6)	2.52 (-8)	1.08 (-6)	1.38 (-6)
S III	6312	8.39(-6)				9.13 (-7)					1.06 (-6)		
Cℓ III	5537	1.09(-8)	1.09(-8)	1.61	1.76 (-8)	1.63 (-8)	1.63 (-8)	1.69	2.75 (-8)	3.50 (-8)	2.27 (-8)	2.27 (-8)	3.85 (-8)
Ar III	7135	1.72(-6)	2.26(-6)	1.0	2.26 (-6)	6.34 (-7)	6.34 (-7)	1.0	6.34 (-7)	1.15 (-6)	8.18 (-7)	8.18 (-7)	8.18 (-7)
Ar IV	4740	5.39(-7)											

*In hypothesis II we assume T_ϵ = 12,000°K for N II and S II, T_ϵ = 9000°K for everything else.

TABLE 13

IONIC CONCENTRATIONS, IONIZATION CORRECTION FACTORS, ABUNDANCES DERIVED FROM MODELS

		NGC 6751					IC 4846				
		$N(X_i)$	$\Sigma N(X_i)$	ICF	N(X)	Model	$N(X_i)$	$\Sigma N(X_i)$	ICF	N(X)	Model
He I		0.102	0.102	1.0	0.102	0.104	0.091	0.091		0.091	0.098
C III	1909						5.32(-5)	5.32(-5)	1.88	1.00(-4)	---
N II	6584	8.37(-5)	8.37(-5)	3.12	2.61(-4)	1.14(-4)	3.38(-6)	3.38(-6)	17.6	5.95(-5)	4.4 (-5)
O II	3727	1.48(-4)	3.98(-4)	1.0	3.98(-4)	3.5 (-4)	2.97(-5)	4.63(-4)	1.0	4.63(-4)	4.00(-4)
O III	4959/5007	2.50(-4)					4.33(-4)				
Ne III	3868	6.79(-5)	6.79(-5)	1.03	7.0 (-5)	7.4 (-5)	6.98(-5)	6.98(-5)	1.01	7.05(-5)	8.5 (-5)
S II	6717/6730	9.78(-7)	4.0 (-6)	1.17	4.7 (-6)	5.0 (-6)	1.91(-7)	2.99(-6)	2.2	6.58(-5)	6.56(-6)
S III	6312	3.02(-6)					2.81(-6)				
Cℓ III	5537	1.70(-7)	1.70(-7)	1.54	2.6 (-7)	2.6 (-7)	6.96(-8)	6.96(-8)	2.5	1.74(-7)	1.40(-7)
Ar III	7135	1.55(-6)	1.55(-6)	1.25	1.94(-6)	1.9 (-6)	7.03(-7)	1.23(-6)	1.0	1.23(-6)	1.80(-6)
Ar IV	4740						5.21(-7)				

TABLE 14

Ionic Concentrations, Ionization Correction Factors, Abundances Derived from Models

		NGC 6778				NGC 6790			Abundance	
		$N(X_i)$	$\Sigma N(X_i)$	ICF	Abundance	$N(X_i)$	$\Sigma N(X_i)$	ICF	N(X)	Model
He I		0.16	0.16	1.0	0.16	0.103	0.103	1.0	0.103	0.104
C III	4267	6.7 (-4):	6.7 (-4):	1.5	1.0 (-3)†	3.44 (-4)	3.44 (-4)	2.0	6.88 (-4)	6.40 (-4)†
N II	6584	1.43(-4)	1.43(-4)	2.25	3.22 (-4)	2.32 (-6)	2.32 (-6)	42	9.74 (-5)	9.35 (-5)
O II	3727	1.36(-4)				1.23 (-5)				
O III	4959/5007	1.70(-4)	3.06(-4)	1.0	3.06 (-4)	3.78 (-4)	3.90 (-4)	1.0	3.90 (-4)	4.02 (-4)
Ne III	3868	1.59(-4)	1.59(-4)	1.6	2.54 (-4)	6.22 (-5)	6.22 (-5)	1.0	6.22 (-5)	8.3 (-5)
S II	6717/6730	2.16(-6)	1.52(-5)	1.0	1.52 (-5)	2.40 (-8)				
S III	6312	1.3 (-5)				1.36 (-6)	1.80 (-6)*	1.18	2.12 (-6)	4.68 (-6)
						0.42 (-6)	(2.57)(-6)		(3.1) (-6)	
S IV	10.5 μ					1.18 (-6)*				
Cℓ II	8577					1.11 (-8)				
Cℓ III	5517/5537	2.40(-7)	2.4 (-7)	1.5	3.6 (-7)	1.60 (-8)	6.27 (-8)	1.12	7.02 (-8)	1.00 (-7)
Cℓ IV	7530/8045					3.56 (-8)				
Ar III	7135	2.05(-6)	2.05(-6)	1.3	2.7 (-6)	2.92 (-7)				
						9.7 (-7)				
	9 μ					5.3 (-7)	1.5 (-6)	1.0	1.5 (-6)	9.2 (-7)
Ar IV	4740					7.1 (-7)				

TABLE 15

Ionic Concentrations, Ionization Correction Factors, Abundances Derived from Models

		NGC 6803				M1 - 74			Abundance	
		$N(X_i)$	$\Sigma N(X_i)$	ICF	Abundance	$N(X_i)$	$\Sigma N(X_i)$	ICF	N(X)	Model
He I		0.127	0.127	1.0	0.127	0.104	0.104	1.0	0.104	0.115
C III	4267	5.18 (-4)	5.18(-4)	1.03	5.36(-4)†	5.83 (-4)	5.83 (-4)	1.77	1.032(-4)†	---
N II	6583	2.97 (-5)	2.97(-5)	10.5	3.12(-4)	1.045(-4)	1.045(-5)	15.4	1.61 (-4)	1.25 (-4)
O II	3727	5.02 (-5)				5.89 (-4)				
O III	4959/5007	5.36 (-4)	5.86(-4)	1.0	5.86(-4)	5.02 (-4)	5.61 (-4)	1.0	5.61 (-4)	4.6 (-4)
Ne II	12.8 μ	4.4 (-5)	2.37(-4)	1.0	2.37(-4)					
Ne III	3868	1.93 (-4)				1.265(-4)	1.265(-4)	1.0	1.27 (-4)	1.35 (-4)
S II	6717/6730	5.41 (-7)				2.67 (-7)	7.19 (-6)	2.04	1.47 (-5)	1.35 (-5)
S III	6312		1.28(-5)	1.0	1.28(-5)	6.92 (-6)				
	9532	6.26 (-6)								
S IV	10.5 μ	6.00 (-6)								
Cℓ III	5517/5537					1.09 (-7)	1.09 (-7)	2.26	2.46 (-7)	2.0 (-7)
Ar III	7135					2.61 (-6)				
	9 μ	6.47 (-6)	8.21(-6)	1.0	8.21(-6)		3.23 (-6)	1.0	3.23 (-6)	6.25 (-6)
Ar IV	4740	1.74 (-6)				6.15 (-7)				

TABLE 16

IONIC CONCENTRATIONS, IONIZATION CORRECTION FACTORS, ABUNDANCES DERIVED FROM MODELS

		NGC 6826					NGC 7026				
					Abundance					Abundance	
		N(X$_i$)	ΣN(X$_i$)	ICF	N(X)	Model	N(X$_i$)	ΣN(X$_i$)	ICF	N(X)	Model
He I		0.106	0.106	1.0	0.106	0.104	0.100	0.101	1.00	0.101	0.117
He II							0.010				
C III	4267	9.85 (-5)	9.85 (-5)	1.8	1.77 (-3)†	1.63 (-3)	8.3 (-4)	8.3 (-4)	1.55	1.28 (-3)	0.85 (-3)†
N II	6583	8.27 (-7)	8.27 (-7)	38.5	3.2 (-5)	2.72 (-5)	3.57 (-5)	3.57 (-5)	7.7	2.75 (-4)	2.2 (-4)
O II	3727	1.0 (-5)	2.41 (-4)	1.0	2.41 (-4)	2.08 (-4)	7.3 (-5)	5.58 (-4)	1.1	6.14 (-4)	5.3 (-4)
O III	4959/5007	2.31 (-4)					4.85 (-4)				
Ne III	3868	9.41 (-5)	9.41 (-5)	1.01	9.50 (-5)	3.92 (-5)	1.62 (-4)	1.62 (-4)	1.13	1.83 (-4)	2.1 (-4)
S II	6717/6730	1.19 (-8)	6.60 (-7)	2.22	1.47 (-6)	1.70 (-6)	0.84 (-6)				
S III	6312	6.48 (-7)					0.7 (-5)	3.6 (-5)	1.10	4.0 (-5)	1.4 (-5)
S III	9069						1.08 (-5)				
S IV	10.5 μ						2.61 (-5)				
Cℓ II	8577						3.8 (-8)				
Cℓ III	5517/5537	5.34 (-8)	5.34 (-8)	2.12	1.13 (-7)	1.00 (-7)	1.47 (-7)	2.94 (-7)	1.13	3.32 (-7)	3.4 (-7)
Cℓ IV	7530/8045						1.09 (-7)				
Ar III	7135	3.74 (-7)	1.11 (-6)	1.0	1.11 (-6)	1.2 (-6)	2.4 (-6)	4.01 (-6)	1.06	4.24 (-6)	5.2 (-6)
Ar IV	4740	7.33 (-7)					1.6 (-6)				

TABLE 17

Ionic Concentrations, Ionization Correction Factors, Abundances Derived from Models

		IC 5117			Abundance		IC 5217			Abundance	
		$N(X_i)$	$\Sigma N(X_i)$	ICF	N(X)	Model	$N(X_i)$	$\Sigma N(X_i)$	ICF	N(X)	Model
He I		0.102	0.110	1.0	0.110		0.088	0.100	1.0	0.100	0.110
He II		0.008					0.012				
C III	4267	4.74 (-4)	4.47 (-4)	1.88	8.9 (-4)	4.0 (-4)†	2.47 (-4)	2.47 (-4)	2.28	5.63 (-4)	5.31 (-4)†
N II	6583	7.0 (-6)	7.0 (-6)	18.7	1.31 (-4)	1.0 (-4)	4.15 (-6)	4.15 (-6)	25.6	1.06 (-4)	1.04 (-4)
O II	3727	3.2 (-5)	3.38 (-4)	1.11	3.75 (-4)	4.43(-4)	1.45 (-5)	3.21 (-4)	1.14	3.66 (-4)	3.60 (-4)
O III	4959/5007	3.06 (-4)					3.06 (-4)				
Ne III	3868	8.17 (-5)	9.13 (-5)	1.02	9.31 (-5)	1.27(-4)	7.21 (-5)	7.21 (-5)	1.16	8.36 (-5)	1.00 (-4)
Ne IV	4724	9.6 (-6)									
S II	6717/6730	8.24 (-8)					1.05 (-7)				
S III	6312	2.45 (-6)	10.3 (-6)	1.18	1.21 (-5)	1.00(-5)	2.30 (-6)	1.33 (-5)	1.28	1.70 (-5)	0.65 (-5)
S III	9069	2.55 (-6)					3.4 (-6)				
S IV	10.5 μ	7.8 (-6)					9.8 (-6)				
Cℓ II	8577	1.16 (-8)									
Cℓ III	5517/5537	2.46 (-8)	1.26 (-7)	1.13	1.43 (-7)	1.47(-7)	5.09 (-8)	1.8 (-7)	1.27	2.29 (-7)	1.70 (-7)
Cℓ IV	7530/8045	9.0 (-8)					1.29 (-7)				
Ar III	7135	7.87 (-7)					6.3 (-7)				
Ar IV	4740	1.20 (-6)	2.03 (-6)	1.02	2.07 (-6)*	2.40(-6)	1.42 (-6)	2.05 (-6)	1.10	2.25 (-6)	2.1 (-6)
Ar V	6435/7005	3.85 (-8)									
K IV	6101	2.75 (-8)	2.75 (-8)	1.21	3.3 (-8)		2.70 (-8)	2.7 (-8)	1.2	3.24 (-8)	

* See notes.

TABLE 18

IONIC CONCENTRATIONS, IONIZATION CORRECTION FACTORS, ABUNDANCES DERIVED FROM MODELS FOR Hb 12

		x	N(X)	ΣN(X)	ICF	N_{total}
He			0.105	0.105	1.0	0.105
C	4267		2.36 (-4)	2.36 (-4)	2.2	5.2 (-4)
N	6583	50	1.11 (-5)	1.11 (-5)	2.1	2.33 (-5)
O II	3727	50	1.18 (-4)	2.54 (-4)	1.0	2.54 (-4)
O III	4959/5007	50	1.36 (-4)			
Ne III	3868	50	3.84 (-5)	3.84 (-5)	1.0	3.9 (-5)
S II	6717/6730	0.8	3.9 (-9)	3.8 (-6)	7	2.7 (-5)
S III	6312	0.8	3.8 (-6)			
Cℓ III	5517/5537	0.8	9.93 (-9)	9.9 (-9)	2.3	2.28 (-8)

TABLE 19

IONIC CONCENTRATIONS, IONIZATION CORRECTION FACTORS, ABUNDANCES DERIVED FROM MODELS

		M 1 - 1				IC 351			
		$N(X_i)$	$\Sigma N(X_i)$	ICF	Abundance	$N(X_i)$	$\Sigma N(X_i)$	ICF	Abundance
He I		0.032	0.117	1.0	0.117	0.048	0.099	1.0	0.099
He II		0.085				0.051			
C III	4267					4.77 (-4)	4.77 (-4)	2.77	1.32 (-3)†
N II	6583	1.208(-6)		39.2	4.8 (-5)	6.35 (-8)	6.35 (-8)	140	0.9 (-5):
O II	3727	1.39 (-6)	5.45 (-5)	3.67	2.0 (-4)	1.88 (-6)	2.22 (-4)	1.38	3.06 (-4)
O III	4959/5007	5.31 (-5)				2.20 (-4)			
Ne III	3868	7.75 (-6)				4.72 (-5)			
Ne IV	4725	3.31 (-5)	7.1 (-5)	1.03	7.3 (-5)	1.97 (-5)	6.77 (-5)	1.01	6.84 (-5)
Ne V	3346/3426	3.05 (-5)				8.03 (-7)			
Na IV	3242	1.8 (-6)			> 2.0 (-6)				
S II	6717/6730	2.85 (-8)	3.03 (-6)	40	1.2 (-4)				
S III	6312	3.0 (-6)				5.35 (-7)	5.35 (-7)	3.9	2.08 (-6):
Cℓ III	5537					1.15 (-8)	1.15 (-8)	2.8	3.2 (-8)
Ar III	7135	1.9 (-7)				0.32 (-6)			
Ar IV	4740	8.8 (-7)	1.84 (-6)	1.7:	3.1 (-5)	1.69 (-6)	2.14 (-6)	1.06	2.27 (-6)
Ar V	6435/7005	7.7 (-7)				0.13 (-6)			
K IV	6101					2.9 (-8)	2.9 (-8)	1.5	4.35 (-8)

TABLE 20

IONIC CONCENTRATIONS, IONIZATION CORRECTION FACTORS, ABUNDANCES DERIVED FROM MODELS

		Hu 1-1 = 119-6°1				IC 1747				
		$N(X_i)$	$\Sigma N(X_i)$	ICF	Abundance	$N(X_i)$	$\Sigma N(X_i)$	ICF	$\Sigma N(X_i)$	Model
He I		0.091	0.106		0.106	0.103	0.111(-4)	1.0	0.111(-3)	0.108
He II		0.015				0.008				
C III	4267					7.28 (-4)	7.28 (-4)	1.72	1.25 (-3)	1.03 (-3)†
N II	6583	4.51 (-5)		3.1	1.40 (-4)	7.12 (-6)	7.12 (-6)	28.6	2.04 (-4)	1.60 (-4)
O II	3727	1.39 (-4)	4.50 (-4)	1.2	5.40 (-4)	2.83 (-5)	5.16 (-4)	1.10	5.66 (-6)	4.83 (-4)
O III	4959/5007	3.11 (-4)				4.88 (-4)				
Ne III	3868	6.90 (-5)	6.90 (-5)	1.31	9.04 (-5)	1.05 (-5)	1.07 (-4)	1.03	1.10 (-4)	1.20 (-4)
Ne IV						2.5 (-6)				
S II	6717/6730	1.06 (-6)	3.69 (-6)	3.65	1.35 (-5)	1.46 (-7)	3.42 (-6)	2.10	7.2 (-6)	1.08 (-5)
S IV	6312	2.63 (-6)				3.27 (-6)				
Cℓ III	5537	6.15 (-8)	6.15 (-8)	2.04	1.25 (-7)	1.11 (-7)	1.11 (-7)	2.01	2.23 (-7)	1.80 (-7)
Ar III	7135	1.21 (-6)	1.64 (-6)	1.10	1.80 (-6)	1.09 (-6)	2.04 (-6)	1.06	2.16 (-6)	2.60 (-6)
Ar IV	4740	4.27 (-7)				9.45 (-7)				

TABLE 21

Ionic Concentrations, Ionization Correction Factors, Abundances Derived from Models

		IC 2003			Abundance		NGC 1535*			Abundance	
		N(Xi)	ΣN(Xi)	ICF	N(X)	Model	N(Xi)	ΣN(Xi)	ICF	N(X)	Model
He I		0.0657	0.0962	1.0	0.096	0.100	0.079	0.094	1.0	0.094	0.108
He II		0.0305					0.015				
C III	4267	4.86 (-4)	4.86 (-4)	1.9	9.23 (-4)	0.81 (-3)†	[1.15 (-3)?]			[1.85(-3)?]	
	1908						1.25 (-4):	1.25 (-4)	2.92	3.65(-4):	4.0 (-4)
N II	6563	5.10 (-6)	5.1 (-6)	21.3	1.09 (-4)	0.7 (-4)	3.9 (-8)		100	>3.9 (-6)?	2.0 (-5)
N III	1747						4.6 (-4)?			<4.6 (-4)?	
O II	3727	1.63 (-5)	2.97 (-4)	1.39	4.12 (-4)	2.65 (-4)	3.34 (-6)				
O III	4959/5007	2.80 (-4)					3.02 (-4)	3.8 (-4)	1.07	4.05(-4)	4.75 (-4)
O IV	1406						7.4 (-5):				
Ne III	3868	5.23 (-5)	7.45 (-5)	1.04	7.75 (-5)	5.8 (-5)	6.58 (-5)	6.58 (-5)	1.26	8.3 (-5)	1.37 (-4)
Ne IV	4725	2.22 (-5)									
S II	6717/6730	1.18 (-7)	1.92 (-6)	2.06	3.95 (-6)	2.56 (-6)					
S III	6312	1.80 (-6)									
Cℓ III	5537	4.67 (-8)		2.66	1.24 (-7)	0.9 (-7)	1.91 (-8)	1.03 (-7)	1.22	1.26 (-7)	1.85 (-7)
Cℓ IV	7530/8045						8.40 (-8)				
Ar III	7135	5.60 (-7)					3.47 (-7)				
Ar IV	4740	1.11 (-6)	1.78 (-6)	1.09	1.94 (-6)	1.2 (-6)	1.35 (-6)	1.7 (-6)	1.14	1.93 (-6)	3.0 (-6)
Ar V	6435/7005	1.09 (-7)									

*The IUE data in NGC 1535 are affected by contributions of the central star.

TABLE 22

IONIC CONCENTRATIONS, IONIZATION CORRECTION FACTORS, ABUNDANCES DERIVED FROM MODELS FOR NGC 2452

			Central Region				S.E. Corner				N.E. Corner		
		$N(X_i)$	$\Sigma N(X_i)$	ICF	Abundance	$N(X_i)$	$\Sigma N(X_i)$	ICF	Abundance	$N(X_i)$	$\Sigma N(X_i)$	ICF	Abundance
He I		0.054	0.117	1.0	0.117	0.072	0.109	1.0	0.109	0.052	0.106	1.0	0.106
He II		0.063				0.037				0.054			
N II	6583	3.04 (-5)		14.5	4.41 (-4)	5.41 (-5)	5.41 (-5)	18.2	9.85 (-4)	3.24 (-5)	3.24 (-5)	15.6	5.05 (-4)
O II	3727	2.14 (-5)	2.74 (-4)	1.40	3.84 (-4)	2.70 (-5)	3.87 (-4)	1.44	5.57 (-4)	3.95 (-5)	4.7 (-4)	1.41	6.63 (-4)
O III	4959/5007	2.53 (-4)				3.60 (-4)				4.30 (-4)			
Ne III	3868	5.07 (-5)	6.1 (-5)	1.30	7.93 (-5)	9.26 (-5)	9.96 (-5)	1.32	1.31 (-4)	6.89 (-5)	6.89 (-5)	1.61	1.11 (-4)
Ne V	3346/3426	1.0 (-5)				0.7 (-5)							
S II	6717/6730	0.75 (-6)	4.04 (-6)	1.92	7.76 (-6)	1.14 (-6)	8.97 (-6)	2.06	1.85 (-5)	6.8 (-7)	6.99 (-6)	1.96	1.37 (-5)
S III	6312	3.29 (-6)				7.82 (-6)				6.3 (-6)			
Cℓ III	5537	6.66 (-8)	6.66 (-8)	2.62	1.74 (-7)	1.18 (-7)	1.18 (-7)	2.74	3.23 (-7)	9.0 (-8)	9.0 (-8)	2.67	2.40 (-7)
Ar III	7135	1.34 (-6)				1.98 (-6)				1.93 (-6)			
Ar IV	4740	1.28 (-6)	2.93 (-6)	1.13	3.31 (-6)	1.52 (-6)	3.81 (-6)	1.13	4.30 (-6)	2.41 (-6)	4.86 (-6)	1.13	5.49 (-6)
Ar V	6435/7005	3.13(-7)				3.14 (-7)				0.52 (-6)			

TABLE 23

IONIC CONCENTRATIONS, IONIZATION CORRECTION FACTORS, ABUNDANCES DERIVED FROM MODELS

NGC 2371 - 2372

			West Lobe				East Lobe		
		$N(X_i)$	$\Sigma N(X_i)$	ICF	Abundance	$N(X_i)$	$\Sigma N(X_i)$	ICF	Abundance
He I		0.063	0.113	1.0	0.113	0.035	0.13	1.0	0.13
He II		0.050				0.094			
C III	4267	1.011(-3)		1.8	1.82 (-3)†				
N II	6583	4.56 (-5)		7.0	3.2 (-4):	1.05 (-5)	1.05 (-5)	20:	2.1 (-4):
O II	3727	7.0 (-5)	5.0 (-4)	1.44	7.20 (-4):	1.03 (-5)	1.993(-4)	3.6	7.2 (-4):
O III	4959/5007	4.3 (-4)				1.89 (-4)			
Ne III	3868	1.00 (-4)		2.02	2.04 (-4):	3.97 (-5)			
Ne V	3346/3426					2.68 (-5)	6.65 (-5)	2.7	1.8 (-4):
S II	6717/6730	1.40 (-6)	9.86 (-6)	1.9	1.87 (-5)	4.14 (-7)	5.91 (-6)	2.54	1.50 (-5)
S III	6312	8.46 (-6)				5.50 (-6)			
Cℓ III	5537	1.53 (-7)	1.53 (-7)	2.5	3.82 (-7)	9.05 (-8)	9.05 (-8)	3.12	2.83 (-7)
Ar III	7135	1.81 (-6)				1.10 (-6)			
Ar IV	4740	2.31 (-6)	4.65 (-6)	1.12	5.2 (-6)	3.18 (-6)	5.57 (-7)	1.15	6.44 (-6)
Ar V	6435/7005	5.27 (-7)				1.29 (-6)			

TABLE 26

IONIC CONCENTRATIONS, IONIZATION CORRECTION FACTORS, ABUNDANCES DERIVED FROM MODELS

		J 900			Abundance		NGC 6818			Abundance	
		$N(X_i)$	$\Sigma N(X_i)$	ICF	N(X)	Model	$N(X_i)$	$\Sigma N(X_i)$	ICF	N(X)	Model
He I		0.060	0.098	1.0	0.098	0.112	0.045	0.107	1.0	0.107	0.113
He II		0.038					0.062				
C III	4267	[9.63 (-4)]					4.93 (-4)				
	1908	7.68 (-4)					2.71 (-4)				
C IV	1487		1.03 (-3)	1.21	1.25 (-3)	1.48 (-3)	2.48 (-5)	2.96 (-4)	1.49	4.41 (-4)	4.7 (-4)
	1549	2.61 (-4)									
C V	4659						<1.51 (-4)				
N II	6583	4.74 (-6)		(12.3)	[5.85 (-5)]		4.03 (-6)				
N III	1747		2.46 (-4):	2	5.0 (-4):	5.0 (-5)	5.07 (-5)	1.29 (-4)	1.07	1.38 (-4)	2.1 (-4)
N IV	1487	1.9 (-4):					7.02 (-5)				
N V	1240	5.1 (-5):					4.14 (-6)				
O II	3727	2.07 (-5)					1.19 (-5)				
O III	4959/5007	2.12 (-4)	2.32 (-4)	1.35	3.14 (-4)	2.50 (-4)	2.87 (-4)	2.98 (-4)	1.87	5.57[3](-4)	5.25 (-4)
	1661/1666	3.9 (-4):					2.49 (-4)				
O IV	1406	< 4 (-4)									
Ne III	3868	4.85 (-5)					4.70 (-5)				
Ne IV	4725	3.2 (-5)	8.13 (-5)	1.01	8.21 (-5)	7.3 (-5)	6.5 (-5)				
	2422	2.6 (-5)						1.30 (-4)	1.0	1.30 (-4)	1.15(-4)
Ne V	3346/3426	0.38 (-5)					1.8 (-5):				
Na IV	3242						1.32 (-6)	1.32 (-6)	2.36	3.12 (-6)	
S II	6717/6730	1.385(-8)	1.30 (-6)	1.86	2.42 (-6)	5.2 (-6)	1.03 (-7)	2.90 (-6)	3.06	8.86 (-6)	1.15(-5)
S III	6312	1.29 (-6)					2.80 (-6)				
Cℓ III	5537	2.4 (-8)	8.5 (-8)	1.44	1.22 (-7)	2.0 (-7)	5.52 (-8)	5.52 (-8)	3.51	1.94 (-7)	1.38(-7)
Cℓ IV	7530/8045	6.1 (-8)									
Ar III	7135	3.05 (-7)	1.05 (-6)	1.12	1.17 (-6)	6.5 (-7)	7.42 (-7)	3.21 (-6)	1.19	3.82 (-6)	3.7 (-6)
Ar IV	4740	6.32 (-7)					1.94 (-6)				
Ar V	6435/7005	1.08 (-7)					5.31 (-7)				
K IV	6101						5.27 (-8)	6.0 (-8)	1.61	9.66 (-8)	9.7 (-8)
K VI	5603						7.28 (-9)				
Ca V	5309						3.51 (-8)	3.51 (-8)	3.23	1.14 (-7)	1.14(-7)

TABLE 25

IONIC CONCENTRATIONS, IONIZATION CORRECTION FACTORS, ABUNDANCES DERIVED FROM MODELS

Ion	λ	IC 2165 N(X_i)	IC 2165 Σ N(X_i)	IC 2165 ICF	IC 2165 Abundance N(X)	IC 2165 Abundance Model	NGC 2022 N(X_i)	NGC 2022 Σ N(X_i)	NGC 2022 ICF	NGC 2022 Abundance
He I		0.053	0.104	1.0	0.104	0.098	0.016	0.107	1.0	0.107
He II		0.051					0.091			
C III	4267	4.66 (-4):								
	1908	3.7 (-4)	8.7 (-4)	1.28	1.11 (-3)	9.2 (-4)	1.03 (-4)			
C IV	1487	6.0 (-4):								
	4650	3.8 (-4):					< 1.13 (-3)	2.71 (-4)	1.29	3.50 (-4)
	1549	1.37 (-4):					1.68 (-4)			
C V	4659	2.2 (-4):								
N II	6583	3.07 (-6)								
N III	1747	4.22 (-5)								
N IV	1487	5.21 (-5)	1.065(-4)	1.05	1.12 (-4)	0.86 (-4)	0.502(-4)	5.02 (-5)	(1.5)	7.53 (-5)
N V	1240	9.15 (-6)								
O II	3727	6.66 (-6)					1.41 (-6)			
O III	4959/5007	1.51 (-4)	1.58 (-4)	1.55	2.45 (-4)	2.9 (-4)	9.34 (-5)	9.48 (-5)	2.06	1.95 (-4)
	1661/1666	1.13 (-4)								
O IV	1406						< 3.25 (-4)			
Ne III	3868	3.16 (-5)					1.85 (-5)			
Ne IV	4725	4.79 (-5)	8.12 (-5)	1.0	8.12 (-5)	8.4 (-5)		1.09 (-4)	1.01	1.10 (-4)
	2422	3.51 (-5)					8.32 (-5)			
Ne V	3346/3426	0.81 (-5)					0.73 (-5)			
Na IV	3242	2.18 (-7)	2.18 (-7)	2.36	5.14 (-7)	[5.7 (-7)]				
S II	6717/6730	0.05 (-6)					1.25 (-8)	1.38 (-6)	23.2	3.21 (-5):
S III	6312	0.68 (-6)	3.7 (-6)	1.5	5.55 (-6)	7.5 (-6)	1.37 (-6)			
	9069	1.15 (-6)								
S IV	10.5 μ	2.5 (-6)								
Cl III	5537	1.89 (-8)	1.01 (-7)	1.57	1.58 (-7)	2.5 (-7)	2.32 (-8)	2.03 (-7)	1.5	3.04 (-7)
Cl IV	7530/8045	8.17 (-8)					1.8 (-7)			
Ar III	7135	2.93 (-7)					0.37 (-6)			
Ar IV	4740	1.15 (-6)	1.743(-6)	1.16	2.02 (-6)	2.6 (-6)	2.01 (-6)	2.94 (-6)	1.12	3.29 (-6)
Ar V	6435/7005	0.30 (-6)					5.57 (-7)			
K IV	6101	2.29 (-8)	2.29 (-8)	2.35	5.4 (-8)		6.04 (-8)	6.04 (-8)	3.46	2.09 (-7)
Ca V	5309	1.94 (-8)	1.94 (-8)	3.62	7.0 (-8)		2.36 (-8)	2.37 (-8)	2	4.74 (-8)

TABLE 26

IONIC CONCENTRATIONS, IONIZATION CORRECTION FACTORS, ABUNDANCES DERIVED FROM MODELS

		J 900			Abundance		NGC 6818			Abundance	
		N(X_i)	ΣN(X_i)	ICF	N(X)	Model	N(X_i)	ΣN(X_i)	ICF	N(X)	Model
He I		0.060	0.098	1.0	0.098	0.112	0.045	0.107	1.0	0.107	0.113
He II		0.038					0.062				
C III	4267	[9.63 (-4)]					4.93 (-4)				
	1908	7.68 (-4)					2.71 (-4)				
C IV	1487		1.03 (-3)	1.21	1.25 (-3)	1.48 (-3)	2.48 (-5)	2.96 (-4)	1.49	4.41 (-4)	4.7 (-4)
	1549	2.61 (-4)									
C V	4659						<1.51 (-4)				
N II	6583	4.74 (-6)		(12.3)	[5.85 (-5)]		4.03 (-6)				
N III	1747						5.07 (-5)				
N IV	1487	1.9 (-4):	2.46 (-4):	2	5.0 (-4):	5.0 (-5)	7.02 (-5)	1.29 (-4)	1.07	1.38 (-4)	2.1 (-4)
N V	1240	5.1 (-5):					4.14 (-6)				
O II	3727	2.07 (-5)					1.19 (-5)				
O III	4959/5007	2.12 (-4)					2.87 (-4)				
	1661/1666	3.9 (-4):	2.32 (-4)	1.35	3.14 (-4)	2.50 (-4)	2.49 (-4)	2.98 (-4)	1.87	5.57[3](-4)	5.25 (-4)
O IV	1406	< 4 (-4)									
Ne III	3868	4.85 (-5)					4.70 (-5)				
Ne IV	4725	3.2 (-5)	8.13 (-5)	1.01	8.21 (-5)	7.3 (-5)	6.5 (-5)				
	2422	2.6 (-5)						1.30 (-4)	1.0	1.30 (-4)	1.15(-4)
Ne V	3346/3426	0.38 (-5)					1.8 (-5):				
Na IV	3242						1.32 (-6)	1.32 (-6)	2.36	3.12 (-6)	
S II	6717/6730	1.385(-8)	1.30 (-6)	1.86	2.42 (-6)	5.2 (-6)	1.03 (-7)	2.90 (-6)	3.06	8.86 (-6)	1.15(-5)
S III	6312	1.29 (-6)					2.80 (-6)				
Cℓ III	5537	2.4 (-8)	8.5 (-8)	1.44	1.22 (-7)	2.0 (-7)	5.52 (-8)	5.52 (-8)	3.51	1.94 (-7)	1.38(-7)
Cℓ IV	7530/8045	6.1 (-8)									
Ar III	7135	3.05 (-7)	1.05 (-6)	1.12	1.17 (-6)	6.5 (-7)	7.42 (-7)				
Ar IV	4740	6.32 (-7)					1.94 (-6)	3.21 (-6)	1.19	3.82 (-6)	3.7 (-6)
Ar V	6435/7005	1.08 (-7)					5.31 (-7)				
K IV	6101						5.27 (-8)	6.0 (-8)	1.61	9.66 (-8)	9.7 (-8)
K VI	5603						7.28 (-9)				
Ca V	5309						3.51 (-8)	3.51 (-8)	3.23	1.14 (-7)	1.14(-7)

1983ApJS...51..211A

TABLE 27

Ionic Concentrations, Ionization Correction Factors, Abundances Derived from Models

		NGC 6905			Abundance		Hu 1-2 (86 − 8°1)			
		$N(X_i)$	$\Sigma N(X_i)$	ICF	N(X)	Model	$N(X_i)$	$\Sigma N(X_i)$	ICF	Abundance
He I		0.022	0.100	1.00	0.100	0.105	0.082	0.160	1.0	0.160
He II		0.078					0.078			
C III	4267						3.49 (-4)			
	1908	8.2 (-5)					4.56 (-5)			
C IV			2.9 (-4)	1.52	4.41 (-4)	4.3 (-4)		9.17 (-5)	1.30	1.19 (-4)
	1549	2.11 (-4)					4.61 (-5)			
C V	4659						2.23 (-4):			
N II	6583	0.732(-6)	[0.73 (-6)]	[40.4]	[0.3 (-4)]:		3.12 (-5)			
N III	1747		1.65 (-4)	2.52	4.2 (-4):	1.0 (-4)	9.27 (-5)	2.60 (-4)	1.22	3.17 (-4)
N IV	1487	1.58 (-4):					1.10 (-4)			
N V	1240						2.6 (-5)			
O II	3727	4.25 (-6)			[7.8 (-4)]		9.79 (-6)			
			1.72 (-4)	2.70	4.65 (-4)	4.55 (-4)				
O III	4959/5007	1.68 (-4)					6.70 (-5)	7.68 (-5)	1.45	1.11 (-4)
	1661/1666	2.61 (-4)								
O IV	1406						< 5 (-5)			
Ne III	3868				[2.0 (-4)]		1.85 (-5)			
Ne IV	4725	4.35 (-5)	4.35 (-5)	3.06	1.33 (-4)	1.50 (-4)	2.2 (-5)	6.76 (-5)	1.0	6.76 (-5)
	2422						3.8 (-5)			
Ne V	3346/3426						1.91 (-5)			
Na IV	3242						4.0 (-8)		5	2.0 (-7)
S II	6717/6730	4.57 (-8)	2.04 (-6)	4.44	9.07 (-6)	1.05 (-5)	3.08 (-7)	1.66 (-6)	1.83	3.04 (-6)
S III	6312	2.0 (-6)					1.35 (-6)			
Cℓ II	8577						1.92 (-8)			
Cℓ III	5537						2.17 (-8)	1.033(-7)	1.48	1.53 (-7)
Cℓ IV	7530/8045						6.24 (-8)			
Ar III	7135	7.37 (-7)					3.34 (-7)			
Ar IV	4740	1.48 (-6)	2.38 (-6)	1.21	2.88 (-6)	3.8 (-6)	6.63 (-7)	1.381(-6)	1.15	1.59 (-6)
Ar V	6435/7005	1.59 (-7)					3.84 (-7)			
K IV	6101						2.17 (-8)	5.3 (-8)	1.0	5.3 (-8)
K V	4163						3.13 (-8):			
Ca V	5309						2.86 (-8)	2.86 (-8)	1.8	5.2 (-8)

For NGC 6905 estimates by Peimbert-Costero procedure are given in square brackets for comparison.

TABLE 28

IONIC CONCENTRATIONS, IONIZATION CORRECTION FACTORS, AND ABUNDANCES DERIVED FROM MODELS

		NGC 6884			Abundance		NGC 7662			
		$N(X_i)$	$\Sigma N(X_i)$	ICF	$N(X)$	Model	$N(X_i)$	$\Sigma N(X_i)$	ICF	Abundance
He I		0.097	0.118	1.0	0.118	0.118	0.059	0.118	1.0	0.118
		0.021					0.059			
C III	4267						7.0 (−4)			
	1908						1.45 (−4)			
C IV	1549	5.18 (−4)	5.18 (−4)	1.66	8.60 (−4)	1.20 (−3)	1.89 (−4)	3.34 (−4)	1.19	3.97 (−4)
C V	4659						[1.35 (−4)]			
N II	6583						5.49 (−7)			
N III	1747	4.12 (−6)	4.12 (−6)	19.2	7.91 (−5)	6.5 (−5)	1.72 (−5)	6.42 (−5)	1.16	7.45 (−5)
N IV	1487						4.65 (−5)			
O II	3727	2.66 (−5)	4.19 (−4)	1.14	4.77 (−4)	4.35 (−4)	2.12 (−6)	3.34 (−4)	1.11	3.70 (−4)
O III	4959/5007	3.92 (−4)					1.62 (−4)			
	1661/1666						1.70 (−4)			
Ne III	3868	8.20 (−5)					3.37 (−5)			
Ne IV	4725	9.62 (−6)	9.16 (−5)	1.03	9.44 (−5)	1.02 (−4)	3.16 (−5)	6.38 (−5)	1.0	6.38 (−5)
	2422						3.0 (−5)			
Ne V	3346/3426						1.85 (−6)			
Na IV	3242						3.63 (−7)	3.63 (−7)	2.13	7.73 (−7)
S II	6717/6730	7.99 (−8)					1.43 (−8)			
	6312	2.20 (−6)	9.17 (−6)	1.15	1.06 (−5)	1.20 (−5)	1.15 (−6)			
S III	9069						1.03 (−6)	4.7 (−6)	1.43	0.67 (−5)
S IV	10.5 μ	6.89 (−6)					3.65 (−6)			
Cℓ II	8583	8.20 (−9)								
Cℓ III	5537	5.14 (−8)	1.886(−7)	1.16	2.19 (−7)	1.90 (−7)	2.93 (−8)			
Cℓ IV	7530/8045	1.29 (−7)					7.84 (−9)	3.71 (−8)	1.41	5.23 (−8)
Ar III	7135	1.34 (−6)					4.36 (−7)			
Ar IV	4740	2.26 (−6)	3.70 (−6)	1.03	3.81 (−6)	3.53 (−6)	1.41 (−6)	2.0 (−6)	1.05	2.10 (−6)
Ar V	6435/7005	1.01 (−7)					1.52 (−7)			
K IV	6101	3.5 (−8)		1.27	4.42 (−8)		4.21 (−8)	4.21 (−8)	1.8	7.58 (−8)
Ca V	5309						1.0 (−8)	1.0 (−8)	3.35	3.3 (−8)

TABLE 29

A.

SUMMARY OF ABUNDANCE DETERMINATIONS, log $(N/N_H)+12$

	NGC 40	Hu 1-1	M 1 - 1	NGC 650-1	IC 1747	IC 351	IC 2003	NGC 1535	J 320	IC 418	NGC 2022	IC 2165
He	> 10.5	11.02[5]B	11.07 B	11.02 B	11.05 A	11.0 A	10.98 A	10.97 A	11.03 A	10.97 B	11.03 A	11.02 A
C				9.08 D†	9.02 B†	9.12 C†	8.97 B†	8.57 D	8.64 D†	8.79 C-†	8.53 C	9.04 B
N	7.99 B	8.15 C	7.7: D	8.56 C-	8.30 B	6.95 D	8.04 B	> 6.6: D	7.6 D	7.87 A	7.88 D	8.05 B
O	8.78 B	8.73 B	8.3: D	8.84 C	8.75 A	8.48 B	8.62 A	8.61 C	8.40 A	8.64 A	8.29 D	8.39 A
Ne	---	7.96 B	7.86:D	8.54 C	8.05 A	7.84 B	7.89 B	7.92 B	7.83 B	7.87 A	8.04 C	7.91 A
S	> 6.6 C	7.13 C	8.08	7.26 D	6.90 B	6.32 C	6.59 C		6.74 C	6.62 A	7.50 C-	6.75 A
Cℓ	> 5.0	5.1 C-			5.34 B	4.5 C	5.10 B	5.10 B	4.52 C	4.94 B	5.48 D	5.20 B
Ar	> 5.8	6.26 C	7.5 D	6.51 C-	6.33 A	6.36 B	6.29 B	6.29 B	6.14 B	6.36 C	6.52 B	6.30 A
Na												5.71 C
K						4.64					5.32 C	4.73 C
Ca											4.67 C	4.85 C
Table	7	20	19	8	20	19	21	21	8	7	25	25
Overall quality	C-	C	C-	C	B+	C	B	B-	C+	A	C+	A

B.

SUMMARY OF ABUNDANCE DETERMINATIONS, log $(N/N_H)+12$

	J 900	NGC 2346	NGC 2371-2372	NGC 2452	NGC 3242	IC 4593	NGC 6210	IC 4634	NGC 6309	NGC 6543	Cn 3 - 1	IC 4776
He	10.99 A	11.24 A	11.08 A	11.05 A-	10.95 A	11.11 A	11.01 B	10.94 A	11.05 B	11.05 A	--	10.93 A
C	9.10 B		9.26 D†		8.43 D			8.13 C†	9.10 D†	9.10 C†	8.7 D-†	
N	7.70 C	8.06 B	8.42 C	8.66 C+	7.91 C	7.10 A-	7.69 B	7.10 B	8.07 C-	7.94 A	7.69 C	7.89 B
O	8.50 B	8.34 B	8.86 C	8.59 B	8.66 A	8.43 A	8.70 A	8.61 A	8.98 C	8.75 A	8.11 D	8.82 A
Ne	7.91 B	7.67 C	8.26 C	7.91 B-	7.85 B	7.53 B	7.98 A	8.00 A	8.10 C	8.15 A	7.93 D	8.05 A
S	6.38 C	6.2 D	7.23 C	6.98 C	6.69 A-	6.77 A	7.33 A	6.60 B	7.52 C	7.0 B	6.4 C-	7.12 B
Cℓ	5.09 C		5.52 C	5.28 C	5.06 B		5.00 C	4.96 C	5.55 C	5.47 B	5.1 D	5.25 B
Ar	6.07 C	6.5 D	6.76 B	6.54 C	6.26 B	5.97 C (6.40)	6.29 C (6.60)	6.15 B	6.76 C	6.42 A		6.35 A
Na					6.03 C							
K					4.52 C				5.26 D			
Table	26	9	23	22	24	9	10	10	24	11	11	12
Overall quality	B-	C	C	C	A	A	A	B	C	A	C-	B+

C.
SUMMARY OF ABUNDANCE DETERMINATIONS, log $(N/N_H)+12$

	Hu 2-1	NGC 6751	IC 4846	NGC 6778	NGC 6790	NGC 6803	MI-74	NGC 6818	NGC 6826	NGC 6884	NGC 6905	NGC 7026
He	10.95 A	11.02 A	10.96 B	11.20 B	11.02 A	11.10 A	11.02 A	11.03 A	11.03 A	11.07 A	11.02 A	11.00 A
C	8.62 B†		9.0 C	9.00 C†	8.82 A†	8.73 C†	9.01 C†	8.65 A	9.23 C†	8.93 A†	8.65 A	9.02 C†
N	7.60 B	8.34 C	7.75 B	8.51 C–	7.98 A	8.50 A	8.11 B	8.15 A	7.47 A	7.86 A	8.00 C	8.40 A
O	8.48 B	8.57 A	8.64 A	8.48 C–	8.60 A	8.77 A	8.71 A	8.74 A	8.38 A	8.66 A	8.66 A	8.79 A
Ne	7.48 B	7.86 A	7.88 A–	8.4 D	7.86 A–	8.37 A	8.11 A	8.09 A	7.98 C	7.99 A	8.15 A	8.28 A
S	6.13 C	6.68 A	6.82 A	7.18 D	6.40 C	7.11 A	7.15 B	6.95 B	6.17 A	7.03 A	7.00 B	7.60 A
Cℓ	4.51 C	5.4 A	5.23 B	5.56 D	4.85 B		5.35 B	5.28 B	5.04 B	5.32 A		5.53 A
Ar	5.90 C	6.28 A	6.09 B	6.43 D	6.17 B	6.91 B	6.54 C	6.58 A	6.05 A	6.57 A	6.46 B	6.63 B
Na								6.49 C				
K								4.99 C		4.65 C		
Ca								5.06 C				
Table	12	13	13	14	14	15	15	26	16	28	27	16
Overall quality	B	A	A–	C–	A	B	A	A	B	A	B	A

D.
SUMMARY OF ABUNDANCE DETERMINATIONS, LOG $(N/N_H)+12$

	IC 5117	Hu 1 - 2	IC 5217	NGC 7662	Hb 12
He	11.04 A	11.20 A	11.0 B	11.07 A	11.02 B
C	8.90 C	8.08 B	8.74 A	8.60 A	8.72 C–
N	8.04 B	8.50 B	8.02 A	7.87 A	7.37 C–
O	8.61 A	8.05 B	8.70 A	8.57 A	8.40 C–
Ne	8.04 A	7.83 B	7.93 A	7.80 A	7.59 C–
S	7.08 A	6.48 B	7.23 B	6.83 A	7.43 C–
Cℓ	5.16 A	5.18 B	5.30 B	4.72 A	4.36 C–
Ar	6.37 A	6.20 B	6.35 B	6.32 A	
Na		5.30 C		5.89 C	
K	4.52 C	4.73 C	4.50 C	4.88 C	
Ca		4.72 C		4.52 C	
Table	17	27	17	28	18
Overall quality	A	B	A–	A	C–

TABLE 30

MEAN COMPOSITIONS OF 38 PLANETARY NEBULAE

	High Excitation				
	This Series	47 Objects	N-Rich	C-Rich	Solar
He	11.04	11.04	11.13	11.03	11.0
C	8.85	8.89	8.72	8.99	8.65
N	8.11	8.26	8.80	8.15	7.96
O	8.62	8.64	8.65	8.69	8.87
F	4.6:	4.6:			4.6:
Ne	8.02	8.03	8.08	8.05	8.05
Na	6.05	6.18			6.28
S	6.99	7.00	6.79	7.09	7.23
Cℓ	5.19	5.22	5.39	5.27	5.5:
Ar	6.40	6.43	6.73	6.46	6.57
K	4.85	4.95	4.93	5.03	5.14
Ca	4.92	5.03	5.17	4.93	6.34

have also studied the abundance of sulfur; such investigations are important because the observed sulfur ionization pattern does not seem to fit theoretical predictions, at least with available models and atomic parameters. It must also be noted that the infrared [Ar III] line at 9 μm tends to yield higher abundances than does the nebular type λ7135 transition. The situation is puzzling and may reflect difficulties in the adopted atomic parameters. Observations on the [Ne II] 12.8 μm line allow a more accurate determination of the neon abundance in low excitation objects such as IC 418.

V. DISCUSSION

Table 29 summarizes the abundances adopted for each nebula. In many instances we have preferred the values derived from the sum of the observed ionic concentrations and ICFs to those found by model representations. In some instances, we take weighted means. The quantity tabulated is $\log(N/N_{\rm H})+12$. For each element we assign a "relative quality" for the determination, subject of course to the underlying assumption of the analysis. The errors, $\Delta \log N$, should be correlated with the letter symbols as follows: "A," $\Delta \log N \lesssim 0.1$; "B," $0.1 < \Delta \log N < 0.2$; "C," $0.2 < \Delta \log N < 0.3$; "C-," $0.3 < \Delta \log N < 0.5$, while "D" means we expect that we have only an order of magnitude.

These numbers are assigned on the basis of the quality of the measured I values and the presumed reliability of the model. In instances where all significant ionization stages are observed, as in some objects studied by Beck *et al.* (1981), the quality of the determination is assigned on the basis of our confidence in the measured intensities and the assumed values of T_ε and N_ε.

If only one stage of ionization of a highly ionized atom is observed, e.g., [K IV], [Na IV], or [Ca V], we have to rely on the model. In such instances we have assigned a grade of "C." We believe that the chief cause of uncertainty is in the model, rather than in the observed values of the line intensities. In Tables 7–28, we have grouped these highly ionized metal ions together.

The [F IV] λ4060 line is observed in a few objects, but we believe that with higher spectral resolution and greater sensitivity, we could obtain both the λ3997 and λ4060 lines in a number of additional objects. In NGC 3242 and NGC 7662 we find $I(\lambda 4060) = 0.11$ and 0.12, respectively. If we assume that $T_\varepsilon = 15{,}000$ K in the F IV zone and that the ionization correction factor is 2.0 on the basis of theoretical models, we get $N(\mathrm{F})/N(\mathrm{H}) \approx 4 \times 10^{-8}$, which agrees with the solar estimate (Ross and Aller 1976). We cannot call this an abundance determination; all we can really say is that the nebular fluorine abundance appears to be consistent with the solar value.

Plots of derived abundances for C, N, O, Ne, S, Cl, and Ar against nebular excitation class (Aller 1956, p. 65) show no dependence of chemical composition on the level of excitation.

Detailed discussion of individual objects, general comparisons with other observers, correlation of abundance with galactic position, etc., are reserved for a second paper now in preparation, but some of the principal results are summarized in Table 30, which pertains only to mean abundances. These mean abundances were calculated in the following way: We assigned weights depending on the quality of the results for each element. Those of quality "A" were assigned a weight of 3; "B" merited a weight of 2; "C," a weight of 1; "C-," a weight of 1/2, and determinations of quality "D" were not included. The logarithms of the weighted averages of elemental abundances on the scale of $\log N(\mathrm{H}) = 12$ for 38 of the 41 objects are given in column (2). We omitted NGC 40, M 1-1 and Cn 3-1, since the overall quality of the nebular results was only "C-."

In the third column we also include data for nine additional nebulae: NGC 2867, 6302, Me 2-1 (Aller *et* *al.* 1981*a*, *b*, *d*), NGC 2392, 6741, 6886 (Aller and Keyes 1980; Aller and Czyzak 1981), and NGC 4361 (Aller *et al.* 1979). These are all high excitation, mostly nitrogen-rich objects. Then in columns (4) and (5) we compare results obtained for high excitation nitrogen and carbon-rich nebulae, respectively (Aller and Czyzak 1981). The last column gives solar abundances adopted from Ross and Aller (1976) and Lambert (1978), as revised for a Santa Cruz workshop (Aller 1980).

The means in columns (1) and (2) are certainly affected by observational selection since planetary nebulae of high surface brightness have been favored. One of the main points of the investigation was to seek trace elements and measure line intensities of faint features. Hence, we have emphasized planetary nebulae of high surface brightness.

The abundance of helium appears to be comparable with that found in the Sun, but the nitrogen-rich objects also tend to be helium-rich objects, as was noted, e.g., by Kaler (1978*a*, *b*, *c*).

Note that the carbon abundance is derived from λ4267 C II, interpreted as a recombination line, or from prominent ultraviolet lines observed with the *IUE*. Observers often have found higher carbon abundances from λ4267 than from the ultraviolet lines (see, e.g., Torres-Peimbert and Peimbert 1977, and references given in the notes on IC 418). From a study of the λ4267 line in 51 planetary nebulae, Kaler (1981) concluded that the median of the distribution of the C/O values is similar to the solar value. In Tables 7–29 we have denoted C abundances derived from λ4267 by a dagger superscript. From 21 planetary nebulae we have found a mean carbon abundance from λ4267, $N(\mathrm{C})/N(\mathrm{H}) = 8.2 \times 10^{-4}$, in good agreement with a value 8.3×10^{-4} reported by French (1980) from permitted C II and C III lines. From nine objects where the carbon abundance is found from the ultraviolet lines we find 6.1×10^{-4}; thus, $\langle \Delta \log N(\mathrm{C}) \rangle = 0.13$ with no significant dependence of the derived N(C) on excitation. The spread of values is about the same. Nevertheless, abundances derived from permitted carbon ion lines seem to show a net residual bias in favor of higher values than do collisionally excited lines. If the permitted lines are excited preferentially in regions of high T_e, dielectronic recombination, which appears to be unimportant at 10,000 K, may play a role. We conclude that, except for the nitrogen-rich objects, carbon tends to be more abundant than in the Sun by a factor of ~1.5 to 2. Note that in our overall sample, nitrogen is also more abundant than in the Sun, but as the reference to Table 29 indicates, there are probably many planetary nebulae that do not have excess N.

Oxygen appears to be invariably less abundant in planetary nebulae than in the Sun, as has been noted by many investigators. The mean abundance of this element and also that of neon seem to be stable among different groups.

Sulfur would appear to be somewhat less abundant than in the Sun. Among the objects studied by Beck *et al.* (1981), $\langle \log N(\mathrm{S}) \rangle = 7.08$, although there appear to be intrinsic fluctuations from object to object.

The solar abundance of chlorine is poorly determined, so we cannot say if there is an actual difference between it and the planetary nebulae. It might be slightly less abundant in the planetary nebulae.

Also, solar and nebular concentrations of argon may be comparable. Possibly argon might be slightly enhanced in nitrogen-rich objects, but temperature uncertainties in the [Ar IV] and [Ar V] zones might account for some of the scatter. Beck *et al.* (1981) find $\langle \log N(\mathrm{Ar}) \rangle = 6.44$.

The data would suggest that the metals sodium and potassium are slightly less abundant than in the Sun, but the scatter is large, and ICFs are also large. It seems certain that calcium is definitely less abundant than in the Sun; i.e., it is systematically depleted in planetary nebulae, perhaps by inclusion in grains (Aller 1978*a*), as is iron in some high excitation planetaries (Shields 1978*a*, *b*).

We are indebted to Dr. C. D. Keyes who assisted in securing all the new ITS observations included in this analysis and who served as trouble shooter for all the reductions of these data. He was also responsible for the successful design and operation of the computer program for theoretical models. We express our gratitude to the Office of Academic Computing, UCLA, for their help and support in all the model calculations. Also, one of us (L.H.A.) expresses his gratitude to the University of Queensland Physics Department for a fellowship during which all the initial diagnostic calculations were carried out. This program was supported in part by NSF grant AST 80-19436 and by NASA: NGS 5383 to UCLA, and by NSF grant AST 76-15727 and NASA: NSG 5-42 to Ohio State University. We are grateful to M. Peimbert, Mrs. S. Torres-Peimbert, M. Perinotto, M. J. Seaton, J. P. Harrington, T. Barker, and Walter Feibelman who supplied us with preprints in advance of publication.

APPENDIX

NOTES ON INDIVIDUAL NEBULAE

NGC 40.—This object is extremely inhomogeneous to as small a scale as can be photographed (see, e.g., Goad 1975). Not surprisingly, the excitation level changes dramatically from point to point, and different sets of observational data cannot be compared since they refer to different filaments and structural details. For example, Minkowski and Aller (1956) did not observe exactly the same region as did Aller *et al.* (1972). The earlier observations appear to pertain to a region of relatively low excitation; the later data pertain to one of medium excitation.

The present series is based primarily on observations secured with the image-tube scanner at the Cassegrain focus on the Shane 3 m telescope at Lick Observatory (AC). In comparing photoelectric and ITS measurements, the only lines we can really collate are the hydrogen lines, since the Balmer decrement is not sensitive to temperature or density within the range presented in NGC 40.

Monochromatic photographs such as those obtained by Goad, or with Holland Ford's image tube at the Cassegrain focus of the Mount Wilson 1.5 m telescope, show that [O III] originates in an inner, high excitation zone, while the radiations of Hα, [N II], and [O II] arise primarily in the outer envelope. The observations we used pertained to this outer lower excitation domain. Sabbadin and Hamzaoglu (1982) found NGC 40 to be an unevenly expanding shell with a mean radius of 15″ and a thickness of 5″.

We tried several schemes, but finally adopted a single combination of density and temperature. We were able to obtain no really satisfactory theoretical model for this object; hence, reliable ICFs could not be derived for helium, chlorine, or argon. The nitrogen abundance should be reliable, since most of the nitrogen atoms are only singly ionized. Likewise, the oxygen abundance should be reasonable. Estimates of sulfur suffer from effects of filamentation, but $n(\mathrm{S})/n(\mathrm{H})$ should be closely $[n(\mathrm{S\ II})+n(\mathrm{S\ III})]/n(\mathrm{H\ II})$. The ionization of helium is probably incomplete.

M1-1 = VV 5 = (130°-11.1).—This appears to be a high excitation object of unusual character. The excessive strength of [Ne V] suggests one of the highest levels of excitation we have observed. AC's measurements appear to be generally in agreement with those of Barker (1978*a*). We tried several constant density models but were unable to secure any kind of a good representation of the line intensities. It is probable that a central star temperature well above 150,000 K will be required. Thus, the central star may belong to Pottasch's (1981) class of high temperature planetary nebulei. At the present time we are not equipped to calculate inhomogeneous models with illuminating stars of such very high temperature.

We adopted a two-temperature scheme with $T_\epsilon = 17{,}000$ K in the zone where radiations of [Ne IV] and [Ne V] are produced. Then ionization correction factors were obtained from a high temperature theoretical model. Further discussion does not seem to be warranted until ultraviolet observations are secured with the *IUE*.

NGC 650-651.—This nebula has a bilaterally symmetrical appearance with a filamentary structure (Aller 1956, p. 240; Sabbadin and Hamzaoglu 1981). For example, large fluctuations in the intensity of [O II] λ3727 are observed. A new series of observations was obtained in 1978 with the ITS.

No theoretical model proved to be adequate, presumably because of the extremely inhomogeneous structure of this nebula. We were able to present the general level of nebular excitation, but not detailed line intensities. The ICF factors are approximate. The nebula shows a complicated internal velocity structure (Taylor 1979).

Hu 1-1.—Measurements by Barker (1978*a*) and AC seemed to be in fair agreement. We have used a two-temperature scheme in analyzing the data. The constant density, ionization-limited, best theoretical model gave the right level of excitation but did not predict line intensities very accurately. It gave ionization correction factors for nitrogen, oxygen, and neon which were very close to those found by the Peimbert-Costero (1969) procedure.

The diagnostic diagram for this nebula strongly suggests that it is rather inhomogeneous and shows an appreciable variation in T_ϵ.

IC 1747.—This is a double-lobed object with a Wolf-Rayet central star. Most of the light of the nebula is contributed by the lobes. Reference to the diagnostic diagram (Fig. 1) suggests that we are dealing with a fairly homogeneous object. The theoretical model (Aller 1982) seems to give a good representation of the observed intensities. The abundances derived from the model and those found by extrapolation from observed ionic concentrations by appropriate ionization correction factors seem to be in good accord.

IC 351.—Newer ITS data obtained in 1978 covering the near-ultraviolet as well as the 5300–6900 Å region are employed in the analysis along with data from Barker (1978*a*), TPP (1978), and AC. We do not observe [S II]; [N II] is extremely weak. Hence, any nitrogen abundance determination will be very uncertain. The theoretical model (Aller 1982) appears to give a reasonably good representation of the line intensities (see also Marionni and Harrington 1981).

IC 2003.—This nebula appears as a small disk with a bright condensation that shows a lower level of excitation than does the rest of the nebula. Intensity values given by Walker and Aller (1965), Barker (1978*a*, *b*, *c*), and TPP (1977) refer to the integrated nebular radiation, while those of AC pertain to the bright condensation. More recently, ITS observations covering the λ3200 to λ4000 region have been obtained. The theoretical model seems to predict the intensities in integrated light fairly well. Compare Marionni and Harrington (1981). Figure 2 gives the diagnostic diagram.

NGC 1535.—This beautifully symmetrical, rather high excitation nebula shows a very narrow range of excitation. Low excitation lines, such as [S II], which often appear in high excitation nebulae are missing. [N II] appears to be barely detectable. The available far-ultraviolet lines observed with the *IUE* all appear to arise from the central star (Feibelman, private communication). We cannot obtain proper abundances for nitrogen and carbon until *IUE* observations avoiding the central star are obtained. The λ4267 line suggests a carbon abundance of 1.85×10^{-3}.

The theoretical model seems to represent the observed intensities fairly well, but the uncertainties appear to be too great to permit a determination of the nitrogen abundance.

J 320.—Additional observations obtained with the ITS and measurements by Barker (1978*a*) and by AC have been analyzed. The available *IUE* measurements probably represent a mixture of stellar and nebular contributions; therefore, they cannot be used to determine carbon and nitrogen abundances. [N II] is relatively weak; the best model suggests ICF = 35. Hence, the nitrogen abundance is poorly determined. Barker's intensity of λ6583 is ~ 40% higher than the value we obtained with the ITS. If we use his $I(6583)$ and our theoretical model, we obtain a nitrogen abundance of 5.6 (−5).

IC 418.—The spectrum of this bright nebula was first studied in detail by Wyse (1942). Our analysis is based on data from Barker (1978*a*, *b*, *c*), TPP (1979), and extensive spectroscopic measurements which are generally in agreement with those of Barker and TPP. The [Ar II] data are from Willner *et al.* (1977). Such discordances as occur can be accounted for by the fact that the ITS observations pertained to the bright ring, while those of Barker and TPP applied to the whole nebula. Scrimger (1979) finds an extinction constant, $C = 0.31$, in good agreement with our result. For the [S III] zone, he finds $T_\varepsilon = 7750$ K. IC 418 has been a favorite subject for builders of empirical three-dimensional models, the most recent of which is that by Reay and Worswick (1979). Theoretical models have been calculated by a number of investigators (e.g., Flower 1968, 1969). We have analyzed the data with the aid of a theoretical model by Aller *et al.* (1980).

Chemical analyses have been carried out by Torres-Peimbert, Peimbert, and Daltabuit (1980) and Harrington *et al.* (1980). The former group finds $\log n(\mathrm{C}) = 9.0$, $\log n(\mathrm{O}) = 8.7$, and $\log n(\mathrm{N}) = 7.9$. Harrington *et al.* call attention to discordances between model predictions and the intensities of λ4267 and ultraviolet carbon lines. They find $\log n(\mathrm{C}) = 8.7 \pm 0.2$. From the ITS measurements of λ4267 and our model, we find $\log n(\mathrm{C}) = 8.79$, but our model also fails to predict correctly the UV lines.

NGC 2022.—The low surface brightness of this nebula makes it a difficult object for investigation. The photoelectric and ITS data of AC seem to agree with those of TPP. Extensive new ITS data in the yellow and near-UV regions have been obtained. New *IUE* data have been obtained by Carpenter and Czyzak (1982) to supplement those supplied by Feibelman (private communication).

We have analyzed the data with the aid of a theoretical model for NGC 4361 (Aller *et al.* 1979), no special model having been calculated for this object.

IC 2165.—The rich spectrum of this object has been studied by many investigators since the pioneering work of Wyse (1942). The adopted value of C = 0.67 and our analysis are based on both ground-based and *IUE* observations. New ITS observations are included. The [Ar III] and [Cl III] diagnostics are poorly established (see Fig. 3). The [N II] and [S II] lines appear to originate in a cooler zone than do the radiations of [O III], [Ne III], etc. From the theoretical model (Aller 1982), we deduce $T_\varepsilon = 15{,}000$ and 18,000 K for the [Ne IV] and [Ne V] zones, respectively. The model appears to be reasonably satisfactory (see also Marionni and Harrington 1981). The central star of IC 2165 was clearly visible on one night of excellent seeing, but no magnitude estimate was possible. Pottasch (1981) assigned $T_s = 322{,}000$ K.

J 900.—This is a nebula of rather high excitation. From the new ITS data we conclude that earlier measurements made by photographic photometry and calibrated photoelectrically (AC) were generally trustworthy. The diagnostics are shown in Figure 4. Although the two sets of *IUE* observations are in good accord, we cannot be sure to what extent the lines which are measured include contributions from the central star, for which Pottasch deduces $T = 235{,}000$ K. For example, we suspect that the UV nitrogen lines come from the central star, since if they were of nebular origin, N III would be prominent. It is not observed. For oxygen, we have used only the [O II] and [O III] lines. For [Ne IV] and [Ne V] we have taken $T_\varepsilon = 15{,}000$ K from the model. For S, Cl, and Ar, the lack of agreement between the model as actually used and the abundances found by the ICF factors is disappointing. The model represented [S II] λλ6717, 30. If the sulfur abundance is modified to represent λ6312 [S III], the discordance is removed. The chlorine abundance was chosen to fit [Cl IV] λ8048; a better compromise would have been to try to fit [Cl III] more closely. If we represent [Ar IV] and [Ar V] rather than [Ar III], the discordance is removed. That is, by choosing to fit different lines, we could have removed the discrepancies entirely! Marked condensations and filamentary structure are probably responsible for these discordances. We conclude that J 900 exhibits an extreme example of the difficulty of trying to represent an inhomogeneous nebula with a homogeneous model.

NGC 2346.—Sabbadin's (1976) measurements of [N II] intensities, but especially of [S II] and [Ar III], are higher than those of AC. We used a theoretical model for NGC 6309 and derived somewhat lower abundances of N, O, and Ne than did Sabbadin. He finds T_ε([N II]) = 14,200 K, as compared with our T_ε([O III]) = 13,200 K.

The bright central star of NGC 2346, classified as A0 III by Calvet and Cohen (1978), is much too cool to excite the nebula. Kohoutek and Senkbeil (1973) postulated a hot companion. On the assumption that this companion has a temperature of 100,000 K, Calvet and Cohen find its radius to be less than 0.1 $R_\odot$. They suggest a total nebular mass of 0.17 $M_\odot$ and a distance of 1700 pc. The bolometric luminosity of the hot star is taken as 90% that of the Sun. Cohen and Barlow (1975) measured an infrared luminosity ~ 42 $L_\odot$, possibly produced by thermal emission from a cloud of hot ($T < 1300$ K) dust grains surrounding the hot component. Mendez, Niemela, and Lee (1978), however, conclude that the bright central star is a foreground object, a horizontal-branch star accidentally superposed on a planetary nebula. The system is puzzling. Kohoutek (1982) finds the nucleus to be an eclipsing variable. Feibelman and Aller (1982) obtained *IUE* observations at various phases of the eclipsing binary nucleus and found substantial changes in the stellar continuum and in the line profiles and intensities. These variations must arise in the central star rather than in the nebula.

NGC 2371–2372.—Our analysis is based entirely on a new set of ITS measurements made in both the west and east lobes. The two lobes appear to have different temperatures, but in each instance the [N II] T_ϵ is less than the [O III] value of T_ϵ. For this very inhomogeneous nebula, wherein the excitation varies markedly from point to point, no fully satisfactory theoretical model could be found. We interpolated in the network of theoretical models approximating the right level of excitation to estimate ICFs. They are therefore very uncertain. For N, O, and Ne, the Peimbert-Costero (1969) procedure would appear to be superior. A compromise was adopted.

NGC 2452.—Curtis' (1918) drawing shows the general appearance of this nebula. Pottasch (1981) assigns $T_s = 185{,}000$ K for the central star which is easily visible in the telescope. ITS measurements had been secured in the central region, and in condensations in the SE and NE corners, respectively. We derived diagnostics for each of these areas and, in order to obtain ICFs, employed a theoretical model which had been calculated originally for IC 2165. The [N II] temperatures seemed to be lower generally than those found for [O III]. For the central region where [Ne V] appeared, we took $T_\epsilon = 15{,}000$ K. The fluctuations in the abundances derived from one part of the nebula to another must represent, in part, the failure of a homogeneous model to represent a structure of many irregularities and the fact that our theoretical models are calculated for the integrated nebular light and not for emission along the line of sight nor for emissions from discrete individual condensations.

NGC 3242.—The TPP, Barker, and AC data are generally in good accord, except for $\lambda 4686$ which is concentrated in the bright ring. New ITS data covering the spectral region $\lambda 3100$–$\lambda 4000$ have been obtained. Feibelman (private communication) notes that the available *IUE* data are affected by the central star. Thus, there is a huge discordance between the carbon abundance deduced from $\lambda 4267$ interpreted as a recombination feature and from $\lambda 1907$ C III, interpreted as a collisionally excited nebular feature. The ionization correction factor for N II is very large and uncertain; the observed *IUE* lines all appear to be of stellar origin. If we use the ionization correction factor of 95 found from the Peimbert-Costero procedure instead of 167, we find $n(\mathrm{N})/n(\mathrm{H}) = 5.3 \times 10^{-5}$, in good agreement with the value found by Wilkes *et al.* (1981). Obviously, observations avoiding the central star are needed.

The best theoretical model indicated $T_\epsilon = 15{,}000$ K in the [Ne IV] zone, leading to a neon abundance of 7.1×10^{-5}. If T_ϵ is as low as 12,000 K, $n(\mathrm{Ne}) = 7.8 \times 10^{-5}$, and the oxygen abundance looks reliable. Most of the sulfur appears as S IV.

IC 4593.—Here we relied mostly on published data, especially of Czyzak, Buerger, and Aller (1975). There is agreement between the results obtained from our theoretical model, which was calculated with a Cassinelli $T(*) = 37396$ K as an interpolation device, and those from Buerger's (1973) model. The largest difference (a factor of 2) is found for neon. The nebular [Ar III] $\lambda 7135$ and the fine structure infrared 9 μm lines give discordant results, viz., 9.3×10^{-7} and 2.5×10^{-6}, respectively.

NGC 6210.—The observational data are adopted from Aller, Czyzak, and Buerger (1970), Barker (1978*a*), Grasdalen (1979), and Beck *et al.* (1981). The theoretical model was computed with a central star flux from Cassinelli (1971) of $T(*) = 37396$; $N_\mathrm{H} = 10{,}000$ cm^{-3} is employed to compute the ionization correction factors. As in IC 4593, the intensity of the infrared argon line is greater than we would expect from $I(\lambda 7135)$.

IC 4634.—New ITS observations are employed to get intensities of lines from $\lambda 3686$ to $\lambda 7751$. The diagnostics suggest T_ϵ([N II]) > T_ϵ([O III]). In order to obtain the ICFs, we employed a theoretical model very similar to that used for NGC 6210, but with a lower density. The helium abundance looks low. Is the ionization complete? The carbon abundance, estimated from $\lambda 4267$, is very uncertain (see Fig. 5).

NGC 6309.—Figure 1 and Table I of Czyzak and Aller (1970) illustrate the difficulties encountered in an observational and theoretical study of this highly stratified, inhomogeneous nebula. Our primary set of observations were those obtained with the ITS in 1977 June for the central region of the nebula; these show high excitation features such as [Ne IV] and [Ne V] (see Fig. 6 for diagnostics). Modeling proved to be difficult. It was not possible to represent all the principal line intensities, but only to reproduce the general level of excitation. Hence, the ICF factors are uncertain.

Feibelman (private communication) reports that the *IUE* data are very disappointing.

Cn 3-1.—This is an extremely low excitation object, which has been analyzed with the aid of a theoretical model (Aller *et al.* 1980). This model predicts $T_\epsilon = 10{,}500$ K, which is somewhat higher than that found by French (1981) and from the [N II] lines. Abundances derived, both by French and in this investigation, are uncertain.

NGC 6543.—The extremely intricate filamentary structure of this well-known bright nebula is well documented in a number of observational studies (Aller and Walker 1970; Czyzak, Aller, and Kaler 1968; Boeshaar 1974; Boeshaar, Czyzak, and Aller 1974; Dopita and Gibbons 1975). Münch (1968) interpreted the extremely complicated kinematical structure of this nebula.

The observed adopted intensities are taken mostly from AC. These data consist of ITS measurements, calibrated with the aid of photoelectric measurements by various observers. We have slightly revised the model given by Aller and Keyes (1980). The abundances derived for most elements seem to be reasonable.

IC 4776.—The observational data were obtained with the ITS in 1978 and 1979 at Lick Observatory. We have employed a standard nebular model based on Cassinelli fluxes for $T(*) = 37396$ K and $N_H = 10{,}000$ cm^{-3}, which appears to be adequate.

Hu 2-1.—A big problem with this nebula was a discordance of the diagnostics; the [N II] lines indicate a high temperature or high density. Barker's observations were in reasonably good agreement with those of AC, except that he obtained T_ε ([N II]) = 10,000 K, while we found 12,000 K. The [O III] measurements gave $T_\varepsilon = 9000$ K. The theoretical model employed to derive the ICF factors is given in Aller (1982).

Analyses were carried out with two hypotheses. In one, we chose $T_\varepsilon = 10{,}000$ K and $\log x = +0.28$ for all ions. In the second hypothesis, we took $T_\varepsilon = 12{,}000$ K for [N II] and [S II], but $T_\varepsilon = 9000$ K otherwise. Thus, the nitrogen abundance is decreased by ~ 33%, the oxygen abundance is increased by 58%, and other elements are generally affected by smaller amounts. The first hypothesis is probably to be preferred. Noskova (1979), however, concludes $N_\varepsilon = 10^4$, $T_\varepsilon = 15{,}000$ K, and he finds the illuminating star to have a flux distribution corresponding to 30,000 K.

The carbon abundance found from λ4267 seems to be in good agreement with that found by Lutz (1981) from *IUE* data.

NGC 6751.—For this nebula a two-temperature model has been assumed, but there appears to be good agreement between abundances found with the aid of the ICF factors and those obtained by a direct theoretical model representation.

IC 4846.—For most lines the agreement between Barker (1978*a*, *b*, *c*) and AC is reasonably good, but the large discordance for [N II] is difficult to understand. In the analysis with the ICF factors, it was assumed that [S II] and [N II] were produced in condensations with $x = 3.1$ and $T_\varepsilon = 10{,}000$ K, while for other ions it was assumed that $x = 0.9$ and $T_\varepsilon = 9700$ K.

The agreement between the model predictions and the ICF method is generally good.

NGC 6778.—This remarkable, rather faint planetary shows marked stratification effects and, more particularly, an unusually strong spectrum of permitted lines of ions of carbon, nitrogen, and oxygen. Observational data from Czyzak and Aller (1973, 1979) have been reassessed with the aid of new ITS measurements. None of the available theoretical models seem to work very well, so the ICF factors are not well determined. The nebula certainly has a high He/H ratio. Presumably, it is also "metal-rich," but although neon and nitrogen seem enhanced above normal values for a planetary nebulae, the abundance of oxygen seems to be low.

NGC 6790.—This bright nebula has been studied by many investigators. Infrared measurements by Beck *et al.* (1981) and Aitken *et al.* (1979) for [Ne II], [Ar III], and [S IV] show some discordances among themselves and with the optical data. The 9.0 [Ar III] line data from Beck *et al.* (1981) give n(S IV) = 0.42×10^{-6}, while those of Aitken *et al.* (1979) give n(S IV) = 1.88×10^{-6}. Then $\Sigma N(X_i) = 1.8 \times 10^{-6}$ and 2.57×10^{-6}, respectively. The 9 μm [Ar III] line gives N(Ar III) = 9×10^{-7} (Beck *et al.*) versus 5.3×10^{-7} (Aitken *et al.*) and 2.92×10^{-7} from [Ar III] λ7135. We have adopted N(Ar III) = 8.5×10^{-7}. The theoretical model (Aller and Keyes 1980) and the general level of excitation all suggest that the λ4686 line originates in the central star and not in the nebula (see Fig. 7).

NGC 6803.—Except for the infrared lines, the observational data are from Lee *et al.* (1974). In particular, N(Ar III) is obtained from the 9 μm line. The theoretical model was based on Cassinelli (T^*) = 37346 K and $N_H = 10{,}000$ cm^{-3}. The ionization correction factors are near 1.0, except for [N II], where it is 10.5.

M1-74.—The agreement between the measurements by Barker (1978*a*) and AC is reasonably good; the data have been reassessed. The theoretical model (Aller and Keyes 1980) originally calculated for $N_H = 6000$ cm^{-3} seems to work well for this object, yielding what appear to be reliable ionization correction factors. The diagnostics are limited, the estimate of N_ε depending almost entirely on the [S II] λ6717/λ6730 ratio.

NGC 6818.—The optical region data are from Aller and Czyzak (unpublished); *IUE* data are those given by Boggess, Feibelman, and McCracken (1981). The model (Aller 1982) seems to predict abundances that are generally in good agreement with those found by use of ICF factors and ionic concentrations. The temperature $T_\varepsilon = 14{,}600$ K in the [Ne IV] zone is obtained by comparing auroral and nebular type transitions. We take $t = 1.25$ for most ions, but for a number of ions we have used the theoretical model to estimate t as follows: C IV, (1.40); N IV, (1.35); N V, (1.60); Ne V, (1.60).

NGC 6826.—Feibelman (1981) describes this as a remarkable triple shell object. The observational data were obtained with the ITS at Lick. The diagnostics are generally in good accord (see Fig. 8). The theoretical model (Keyes and Aller 1980) predicts abundances mostly in reasonable agreement with those found from ionic concentrations and ICF factors.

NGC 6884.—This nebula has a rather rich spectrum of medium to moderately high excitation. The temperature in the [Ne IV] zone is taken from the theoretical model (Aller 1982) which gives abundances in good agreement with those found from ionic concentrations and ICF factors. For diagnostics see Figure 9. Pottasch (1981) suggests T_s = 190,000 K.

NGC 6905.—The AC line intensity measurements were made in the brightest part of a rather inhomogeneous ring. The *IUE* data probably include significant contributions from the central star. Carbon and nitrogen abundances estimated from these lines are therefore very uncertain. Oxygen, neon, sulfur, and argon are probably correct.

NGC 7026.—This is a binuclear nebula with a Wolf-Rayet central star which evidently contains numerous condensations. It is expanding in a complex fashion; the emission appears to come from localized material almost symmetrically placed with respect to the central star (Sabbadin and Hamzaoglu 1982). Although the model gives the right level of excitation, the detailed fit to individual lines was not entirely satisfactory. In particular, the [S II] and [S III] λ6312 lines could not be well reproduced. On the other hand, the [S IV] 10.5 μm line was observed by Beck *et al.* (1981), so the total sulfur abundance is obtained by assuming $n(\mathrm{S}) = n(\mathrm{S\ II}) + n(\mathrm{S\ III}) + n(\mathrm{S\ IV})$. For other elements, the discordances lie within the "normal" range, and for them the agreement is reasonably good. For diagnostics see Figure 10.

IC 5117.—This appears to be an unusually dense nebula. The 9 μm [Ar III] data by Beck *et al.* (1981) give $n(\mathrm{Ar\ III}) = 1.35 \times 10^{-6}$ and $n(\mathrm{Ar}) = 2.4 \times 10^{-6}$. The weak [S II] lines give an uncertain $\log x$ determination. The theoretical model computed for $N_\mathrm{H} = 20{,}000\ \mathrm{cm}^{-3}$ represents well the intensities, but the [N II] and [O III] line ratios suggest a yet higher density. The quality of the abundance determination seems to be good.

Hu 1-2 = (86-8°1).—This nebula shows a very large range in ionization and excitation. There appear to be prominent low excitation, dense condensations. Hence, the construction of a satisfactory theoretical model is difficult, particularly if one is constrained to use a model of constant density. The one that approached most closely the observed distribution of ions gave a bimodal ionization pattern, a consequence of an effort to represent lines of widely different excitation, e.g., [Cl II] and [Ne V].

This nebula is certainly helium rich (see Kaler 1974). The carbon result is based only on the *IUE* data; optical line intensities would imply a somewhat larger abundance. Most of the nitrogen is in higher stages of ionization than N II; we rely here on the *IUE* data. From the model we assume $t(\mathrm{N\ IV}) = 1.6$; $t(\mathrm{N\ V}) = 1.8$. We assume that all the oxygen appears as O II, O III, and O IV. The O IV, λ1403/λ1409 line is blended with silicon; also, $t(\mathrm{O\ IV})$, here estimated as 1.8 or 2.0 from the model, is uncertain. We took $t(\mathrm{Ne\ IV}) = 1.6$ and $t(\mathrm{Ne\ V}) = 1.8$. The ionization correction factors are uncertain for Na, K, and Ca. With sulfur, chlorine, and argon, where several ionization stages are observed, the influence of uncertainties in the ICFs should be small.

The overall conclusion is that helium and nitrogen are certainly overabundant, but that neon and oxygen are probably relatively less abundant than in other nebulae (see also Marionni and Harrington 1981).

IC 5217.—The agreement between the measurements of TPP, Barker, and of AC seem satisfactory. Diagnostic criteria give reasonably consistent results (see Fig. 11). Although the theoretical model represents the observed intensities in a satisfactory way, the model abundances do not agree with those found from the ICF factors as closely as one would like. Different ions of sulfur, chlorine, and argon suggest different abundances.

NGC 7662.—This intensively studied nebula has been analyzed in great detail recently by Harrington, *et al.* (1982). Other investigations have been carried out by Peña and Torres-Peimbert (1981) and Benvenuto and Perinotto (1981). We assumed a theoretical model similar to that developed for NGC 3242. Figure 12 shows the diagnostics. Except for helium, the derived abundances agreed reasonably well with those found by Harrington *et al.* for their Model I. When dust is included (their Model II), the agreement is less satisfactory. For example, more carbon is found since C IV λ1550 is weakened by absorption, and the overall agreement of their model with observed intensities is improved.

In addition to the ultraviolet data of Harrington, Seaton, and Lutz (1979) presented at the London *IUE* conference, and optical region data from a number of observers (see AC and references therein), we have utilized new ITS measurements covering the region λ3100–λ4000.

Our helium abundance agrees with that of Kaler (1980). Our measurements of λλ4686, 5411, and 4541 give consistently $n(\mathrm{He}^{++}) = 0.059$, those of λλ4471, 5776 and 6678 also give 0.059, both for the bright ring. From the integrated light of the nebula, Kaler finds $n(\mathrm{He\ I}) = 0.077$ and $n(\mathrm{He}^{++}) = 0.041$.

Our abundances are generally less than those found by Peña and Torres-Peimbert or Benvenuto and Perinotto, although we find more nitrogen than the latter group found.

Hb 12.—This dense nebula, which was included almost as an afterthought on a 1943–1945 photographic survey of nebular spectra (Aller 1951), turns out to be a very interesting, although seemingly complicated, object. Much effort was wasted in endeavors to construct a uniform density model for this object. Ionic lines of N, O, and Ne appear to be produced in a very dense zone, while [S II] indicates $x \approx 0.35$! Measurements by Barker and by AC appear to be in fair agreement.

REFERENCES

Aitken, D. K., Roche, P. F., Spenser, P. M., and Jones, B. 1979, *Ap. J.*, **233**, 925.
Aller, L. H. 1951, *Ap. J.*, **113**, 125.
______. 1956, in *Gaseous Nebulae* (London: Chapman-Hall), p. 241.
Aller, L. H. 1976, *Pub. Astr. Soc. Pacific*, **88**, 574.
______. 1978*a*, in *IAU Symposium 76, Planetary Nebulae Observations and Theory*, ed. Y. Terzian (Dordrecht: Reidel), p. 225.
______. 1978*b*, *Pub. Astr. Soc. Australia*, **3**, 213.
______. 1980, unpublished.

Aller, L. H. 1982, *Ap. Space Sci.*, **83**, 225.
Aller, L. H., and Czyzak, S. J. 1979, *Ap. Space Sci.*, **62**, 397 (AC).
______. 1981, *Proc. Nat. Acad. Sci.*, **78**, 5266.
Aller, L. H., Czyzak, S. J., and Buerger, E. 1970, *Ap. J.*, **162**, 783.
Aller, L. H., Czyzak, S. J., Buerger, E. G., and Lee, P. 1972, *Ap. J.*, **172**, 361.
Aller, L. H., and Epps, H. W. 1976, *Ap. J.*, **204**, 445.
Aller, L. H., and Keyes, C. D. 1980, *Proc. Nat. Acad. Sci.*, **77**, 1231.
Aller, L. H., Keyes, C. D., and Czyzak, S. J. 1981, *Ap. J.*, **250**, 596.
Aller, L. H., Keyes, C. D., Ross, J. E., and Czyzak, S. J. 1980, *Ap. Space Sci.*, **67**, 349.
Aller, L. H., Keyes, C. D., Ross, J. E., and O'Mara, B. J. 1981*a*, *M.N.R.A.S.*, **197**, 95.
______. 1981*b*, *M.N.R.A.S.*, **197**, 647.
______. 1981*c*, *M.N.R.A.S.*, **194**, 613.
Aller, L. H., Ross, B. J., Keyes, C. D., and Czyzak, S. J. 1979, *Ap. Space Sci.*, **64**, 347.
Aller, L. H., and Walker, M. F. 1970, *Ap. J.*, **161**, 917.
Balick, B. 1975, *Ap. J.*, **201**, 705.
Barker, T. 1978*a*, *Ap. J.*, **219**, 914.
______. 1978*b*, *Ap. J.*, **220**, 193.
______. 1978*c*, *Ap. J.*, **221**, 145.
______. 1980, *Ap. J.*, **240**, 99.
______. 1982, *Ap. J.*, **253**, 167.
Beck, S. C., Lacy, J. H., Townes, C. H., Aller, L. H., Geballe, T. R., and Baas, F. 1981, *Ap. J.*, **249**, 592.
Becker, S. A., and Iben, I. 1980, *Ap. J.*, **237**, 111.
Benvenuto, P., and Perinotto, M. 1981, *Astr. Ap.*, **95**, 127.
Boeshaar, G. O. 1974, *Ap. J.*, **187**, 283.
Boeshaar, G. O., Czyzak, S. J., and Aller, L. H. 1974, *Ap. J. Suppl.*, **28**, 335.
Boggess, A., Feibelman, W., and McCraken, C. W. 1981, in *Universe at Ultraviolet Wavelengths*, ed. R. D. Chapman (NASA Conf. Pub. 2171), p. 663.
Bowen, I. S., and Wyse, A. B. 1939, *Lick Obs. Bull.*, **19**, 1.
Buerger, E. G. 1973, *Ap. J.*, **160**, 887.
Calvet, N., and Cohen, M. 1978, *M.N.R.A.S.*, **182**, 687.
Carpenter, K. G., and Czyzak, S. J. 1982, *Ap. Space Sci.*, **84**, 495.
Cassinelli, J. P. 1971, *Ap. J.*, **165**, 265.
Che, A., and Köppen, J. 1981, preprint.
Cohen, M., and Barlow, M. J. 1974, *Ap. J.*, **193**, 401.
Curtis, H. D. 1918, *Lick Obs. Pub.*, **13**, 1.
Czyzak, S. J., and Aller, L. H. 1970, *Ap. J.*, **162**, 495.
______. 1973, *Ap. J.*, **181**, 817.
______. 1979, *M.N.R.A.S.*, **188**, 229.
Czyzak, S. J., Aller, L. H., and Kaler, J. B. 1968, *Ap. J.*, **154**, 543.
Czyzak, S. J., Buerger, E. G., and Aller, L. H. 1975, *Ap. J.*, **198**, 431.
Czyzak, S. J., Sonneborn, G., Aller, L. H., and Shectman, S. A. 1980, *Ap. J.*, **241**, 719.
Dinerstein, H. 1980, *Ap. J.*, **237**, 486.
Dopita, M. A., and Gibbons, A. H. 1975, *M.N.R.A.S.*, **171**, 73.
Dufour, R. J., and Killen, R. M. 1977, *Ap. J.*, **211**, 68.
Feibelman, W. A. 1981, *Pub. Astr. Soc. Pacific*, **93**, 719.
Feibelman, W. A., and Aller, L. H. 1982, in preparation.
Flower, D. R. 1968, *Ap. Letters*, **2**, 205.
______. 1969, *M.N.R.A.S.*, **146**, 171.
French, H. 1980, *Bull. AAS*, **12**, 842.
______. 1981, *Ap. J.*, **246**, 434.
Goad, L. 1975, Ph.D. thesis, Harvard University.
Grasdalen, G. 1979, *Ap. J.*, **229**, 587.
Harrington, J. P., Lutz, J. H., Seaton, M. J., and Strickland, D. J. 1980, *M.N.R.A.S.*, **191**, 13.
Harrington, J. P., Seaton, M. J., Adam, S., and Lutz, J. H. 1982, *M.N.R.A.S.*, **199**, 517.
Harrington, J. P., Seaton, M. J., and Lutz, M. J. 1979, preprint.
Hawley, S. A., and Miller, J. S. 1977, *Ap. J.*, **212**, 94.
Hummer, D. S., and Mihalas, D. 1970, *M.N.R.A.S.*, **147**, 339.
Kaler, J. B. 1974, *Ap. J. (Letters)*, **188**, L15.
______. 1976, *Ap. J. Suppl.*, **31**, 517.
Kaler, J. B. 1978*a*, *Ap. J.*, **225**, 527.
______. 1978*b*, *Ap. J.*, **226**, 947.
______. 1978*c* in *IAU Symposium 76, Planetary Nebulae Observations and Theory*, ed. Y. Terzian (Dordrecht: Reidel), p. 235.
______. 1979, *Ap. J.*, **228**, 163.
______. 1980, *Ap. J.*, **239**, 78.
______. 1981, *Ap. J.*, **249**, 201.
Keyes, C. D., and Aller, L. H. 1978, *Ap. Space Sci.*, **59**, 91.
______. 1980, *Ap. Space Sci.*, **72**, 203.
Kohoutek, L. 1982, *IAU Circ.*, No. 3667.
Kohoutek, L., and Senkbeil, G. 1973, *Mem. Soc. Roy. Sci. Liege*, 6th series, **5**, 485.
Köppen, J. 1979, *Astr. Ap. Suppl.*, **35**, 111.
Köppen, J., and Tarafdar, S. P. 1978, *Astr. Ap.*, **69**, 363.
Lambert, D. L. 1978, *M.N.R.A.S.*, **182**, 249.
Lee, P., Aller, L. H., Kaler, J. B., and Czyzak, S. J. 1974, *Ap. J.*, **192**, 159.
Lutz, J. 1981, *Ap. J.*, **247**, 144.
Maran, S., Aller, L. H., Gull, T., and Stecher, T. 1982, *Ap. J. (Letters)*, **253**, L43.
Marionni, P. A., and Harrington, J. P. 1981, in *The Universe at Ultraviolet Wavelengths*, ed. R. D. Chapman (NASA Conf. Pub. 2171), p. 633.
Mendez, R., Niemela, V., and Lee, P. 1978, *M.N.R.A.S.*, **184**, 351.
Minkowski, R., and Aller, L. H. 1956, *Ap. J.*, **124**, 93.
Miller, J. S. 1969, *Ap. J.*, **157**, 1215.
Münch, G. 1968, in *IAU Symposium 34, Planetary Nebulae*, ed. C. R. O'Dell and D. E. Osterbrock (Dordrecht: Reidel), p. 259.
Noskova, R. J. 1979, *Astrofizika*, **15**, 631.
Osmer, P. 1976, *Ap. J.*, **203**, 352.
Osterbrock, D. E. 1974, *Astrophysics of Gaseous Nebulae* (San Francisco: Freeman).
Peimbert, M. 1973, *Mem. Soc. Roy. Sci. Liège*, 6th series, **5**, 407.
______. 1978, in *IAU Symposium 76, Planetary Nebulae Observations and Theory*, ed. Y. Terzian (Dordrecht: Reidel), p. 215.
______. 1981, in *Physical Processes in Red Giants*, ed. I. Iben and A. Renzini (Dordrecht: Reidel), p. 409.
Peimbert, M., and Costero, R. 1969, *Bol. Obs. Tonantzintla y Tacubaya*, **5**, 3.
Peimbert, M., and Serrano, A. 1980, *Rev. Mexicana Astr. Ap.*, **5**, 9.
Peña, M., and Torres-Peimbert, S. 1981, *Rev. Mexicana Astr. Ap.*, **6**, 309.
Perek, L., and Kohoutek, L. 1967, *Catalogues of Galactic Planetary Nebulae* (Czechoslovak Academy of Sciences).
Pottasch, S. R. 1981, *Astr. Ap.*, **94**, L13.
Reay, N. K., and Worswick, S. P. 1979, *Astr. Ap.*, **72**, 31.
Renzini, A., and Voli, M. 1981, *Astr. Ap.*, **94**, 175.
Ross, J. E., and Aller, L. H. 1976, *Science*, **9**, 1223.
Sabbadin, F. 1976, *Astr. Ap.*, **52**, 291.
Sabbadin, F., and Hamzaoglu, E. 1981, *M.N.R.A.S.*, **197**, 363.
______. 1982, *Astr. Ap.*, **109**, 131.
Seaton, M. J. 1978, *M.N.R.A.S.*, **185**, 5P.
______. 1979, *M.N.R.A.S.*, **187**, 73P.
Scrimger, J. N. 1979, *J. R.A.S. Canada*, **73**, 90.
Shields, G. 1978*a*, *Ap. J.*, **219**, 565.
______. 1978*b*, *Ap. J.*, **219**, 559.
Shields, G., Aller, L. H., Keyes, C. D., and Czyzak, S. J. 1981, *Ap. J.*, **248**, 569.
Taylor, K. 1979, *M.N.R.A.S.*, **189**, 511.
Torres-Peimbert, S., and Peimbert, M. 1977, *Rev. Mexicana Astr. Ap.*, **2**, 181.
Torres-Peimbert, S., Peimbert, M., and Daltabuit, E. 1980, *Ap. J.*, **238**, 133.
Walker, M. F., and Aller, L. H. 1965, *Ap. J.*, **141**, 1318.
Wilkes, B. J., Ferland, G. J., Hanes, D., and Truran, J. W. 1981, *M.N.R.A.S.*, **197**, 1.
Willner, S. P., Jones, B., Puetter, R. C., Russell, R. W., and Soifer, B. 1977, *Ap. J.*, **234**, 496.
Wyse, A. B. 1942, *Ap. J.*, **95**, 356.

LAWRENCE H. ALLER: Department of Astronomy, University of California, Los Angeles, Los Angeles, CA 90024

STANLEY J. CZYZAK: Astronomy Department, Ohio State University, Columbus, OH 43210